Tran-SET

Transportation Consortium of South-Central States

Solving Emerging Transportation Resiliency, Sustainability, and Economic Challenges through the Use of Innovative Materials and Construction Methods: From Research to Implementation

Coastal Bridges under Hurricane Stresses along the Texas and Louisiana Coast

Project No. 17STTSA02

Lead University: University of Texas at San Antonio

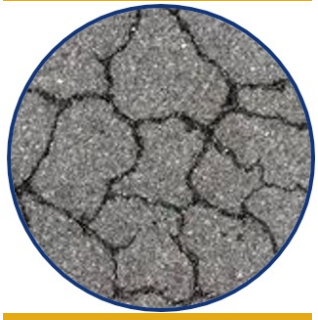

Enhancing Durability and Service Life of Infrastructure

Final Report

December 2018

Disclaimer

The contents of this report reflect the views of the authors, who are responsible for the facts and the accuracy of the information presented herein. This document is disseminated in the interest of information exchange. The report is funded, partially or entirely, by a grant from the U.S. Department of Transportation's University Transportation Centers Program. However, the U.S. Government assumes no liability for the contents or use thereof.

Acknowledgments

The support of the Transportation Consortium of South-Central States (Tran-SET) and the Department of Civil Engineering at the University of Texas at San Antonito is gratefully acknowledged. The authors would like to express their gratitude to Alicia Elmore and Eric Sammarco for contributing valuable time to the assessment of the research effort.

TECHNICAL DOCUMENTATION PAGE

1. Project No.	2. Government Accession No.	3. Recipient's Catalog No.
17STTSA02		

4. Title and Subtitle	5. Report Date
Coastal Bridges under Hurricane Stresses along the Texas and Louisiana Coast	Dec. 2018
	6. Performing Organization Code

7. Author(s)	8. Performing Organization Report No.
PI: Adolfo Matamoros https://orcid.org/0000-0002-5312-7764 Co-PI: Firat Testik https://orcid.org/0000-0002-1259-0162 GRA: Reza Nasouri https://orcid.org/0000-0001-7232-9372 Arturo Montoya https://orcid.org/ 0000-0003-1429-5105	

9. Performing Organization Name and Address	10. Work Unit No. (TRAIS)
Transportation Consortium of South-Central States (Tran-SET) University Transportation Center for Region 6 3319 Patrick F. Taylor Hall, Louisiana State University, Baton Rouge, LA 70803	**11. Contract or Grant No.** 69A3551747106

12. Sponsoring Agency Name and Address	13. Type of Report and Period Covered
United States of America Department of Transportation Research and Innovative Technology Administration	Final Research Report May 2017 – May 2018
	14. Sponsoring Agency Code

15. Supplementary Notes

Report uploaded and accessible at: Tran-SET's website (http://transet.lsu.edu/)

16. Abstract

The main objective of this study is to develop a high-resolution model capable of simulating the response of bridge structures to hydrodynamic loads for hurricane design conditions (i.e., surge height, wave height, and frequency) expected in the Texas-Louisiana coast. The model relied on Coupled Eulerian-Lagrangian (CEL) techniques where solids are simulated with Lagrangian meshes, while fluids are simulated using Eulerian meshes, and was calibrated using historical data from wave impact laboratory tests. Two high resolution models were created, the first of a tsunami wave impact test conducted at Oregon State University and the second of a bridge located in the Gulf Coast that was heavily impacted by hurricane Katrina. The tsunami wave impact model showed that the CEL technique could provide accurate estimates of wave elevation, water velocity, and wall reaction recorded during the tests at Oregon State University. The bridge model was used to calculate bridge support demands for a representative combination of storm surge, wave velocity and wave length.

A parametric study showed that for waves with similar characteristics to those from past hurricanes in the Gulf Coast, calculated connection forces were significantly different for models in which the bridge substructure was included than in models with the common assumption of rigid substructure. Furthermore, the simulations showed that the difference between connection forces calculated with models with rigid and flexible substructure varied for different types of hydrodynamic loading. The findings of this study indicate that it is important to develop a better understanding of the relationship between wave characteristics and dynamic response of the bridge structure before accurate relationships for wave impact forces can be proposed.

17. Key Words	18. Distribution Statement
Eulerian, Lagrangian, Hurricane, Bridge, Wave Impact	No restrictions.

19. Security Classif. (of this report)	20. Security Classif. (of this page)	21. No. of Pages	22. Price
Unclassified	Unclassified	47	

Form DOT F 1700.7 (8-72) **Reproduction of completed page authorized.**

SI* (MODERN METRIC) CONVERSION FACTORS

APPROXIMATE CONVERSIONS TO SI UNITS

Symbol	When You Know	Multiply By	To Find	Symbol
		LENGTH		
in	inches	25.4	millimeters	mm
ft	feet	0.305	meters	m
yd	yards	0.914	meters	m
mi	miles	1.61	kilometers	km
		AREA		
in^2	square inches	645.2	square millimeters	mm^2
ft^2	square feet	0.093	square meters	m^2
yd^2	square yard	0.836	square meters	m^2
ac	acres	0.405	hectares	ha
mi^2	square miles	2.59	square kilometers	km^2
		VOLUME		
fl oz	fluid ounces	29.57	milliliters	mL
gal	gallons	3.785	liters	L
ft^3	cubic feet	0.028	cubic meters	m^3
yd^3	cubic yards	0.765	cubic meters	m^3
		NOTE: volumes greater than 1000 L shall be shown in m^3		
		MASS		
oz	ounces	28.35	grams	g
lb	pounds	0.454	kilograms	kg
T	short tons (2000 lb)	0.907	megagrams (or "metric ton")	Mg (or "t")
		TEMPERATURE (exact degrees)		
^oF	Fahrenheit	5 (F-32)/9 or (F-32)/1.8	Celsius	^oC
		ILLUMINATION		
fc	foot-candles	10.76	lux	lx
fl	foot-Lamberts	3.426	candela/m^2	cd/m^2
		FORCE and PRESSURE or STRESS		
lbf	poundforce	4.45	newtons	N
lbf/in^2	poundforce per square inch	6.89	kilopascals	kPa

APPROXIMATE CONVERSIONS FROM SI UNITS

Symbol	When You Know	Multiply By	To Find	Symbol
		LENGTH		
mm	millimeters	0.039	inches	in
m	meters	3.28	feet	ft
m	meters	1.09	yards	yd
km	kilometers	0.621	miles	mi
		AREA		
mm^2	square millimeters	0.0016	square inches	in^2
m^2	square meters	10.764	square feet	ft^2
m^2	square meters	1.195	square yards	yd^2
ha	hectares	2.47	acres	ac
km^2	square kilometers	0.386	square miles	mi^2
		VOLUME		
mL	milliliters	0.034	fluid ounces	fl oz
L	liters	0.264	gallons	gal
m^3	cubic meters	35.314	cubic feet	ft^3
m^3	cubic meters	1.307	cubic yards	yd^3
		MASS		
g	grams	0.035	ounces	oz
kg	kilograms	2.202	pounds	lb
Mg (or "t")	megagrams (or "metric ton")	1.103	short tons (2000 lb)	T
		TEMPERATURE (exact degrees)		
^oC	Celsius	1.8C+32	Fahrenheit	^oF
		ILLUMINATION		
lx	lux	0.0929	foot-candles	fc
cd/m^2	candela/m^2	0.2919	foot-Lamberts	fl
		FORCE and PRESSURE or STRESS		
N	newtons	0.225	poundforce	lbf
kPa	kilopascals	0.145	poundforce per square inch	lbf/in^2

TABLE OF CONTENTS

LIST OF FIGURES

LIST OF TABLES

ACRONYMS, ABBREVIATIONS, AND SYMBOLS

AASHTO	American Association of State Highway and Transportation Officials
CEL	Coupled Eulerian-Lagrangian
CFD	Computational Fluid Dynamics
DOT	Department of Transportation
FE	Finite Element
NOAA	National Oceanic and Atmospheric Administration
OSU	Oregon State University
SPH	Smoothed Particle Hydrodynamics
UTSA	University of Texas at San Antonio

EXECUTIVE SUMMARY

According to estimates by the National Oceanic and Atmospheric Administration (NOAA) the annualized cost of hurricane damage in the US is approximately $10 billion per year, with a large percentage of that cost attributed to damage in the Gulf of Mexico coastal region. While the US government has made a significant investment to mitigate the risk of earthquakes, the investments to improve resiliency to hurricanes has lagged significantly behind.

The risk to transportation infrastructure associated with large storms in the Gulf of Mexico is very high. For example, researchers estimate the cost of repairing and replacing bridges damaged during hurricane Katrina exceeded $1 billion. State department of transportation (DOT) damage inspection reports after hurricane Katrina showed that the most common type of severe damage caused by the hurricane was superstructure collapse from unseating of the deck, due to the combined actions of storm surge and hydrodynamic forces from waves.

The main objective of this study is to evaluate a new generation of modeling methodologies for fluid-structure interaction and develop a high-resolution finite element (FE) model capable of simulating the response of bridge structures to hydrodynamic loads from hurricane conditions (i.e., surge height, wave height, and frequency) expected in the Texas-Louisiana coast. The focus on the research was on the use of methodologies capable of modeling the coupled response of bridge structures during wave impact, because recent experimental studies *(1)* have shown that substructure flexibility plays an important role on the magnitude of the hydrodynamic forces. This effect has not been properly studied in past research. The FE bridge model was calibrated using data from physical tests and past hurricanes (hurricane Katrina) as described below.

Several FE models were developed with different levels of complexity. The simplest models consisted of waves impacting a bridge pier and bridge girders, and were developed with the following goals: selecting a suitable analysis method and developing confidence on the simulation of waves, the proper definition of boundary conditions, and the modeling of solid-fluid interaction during wave impact.

Two larger FE models were developed in this study. The first was a model of a flume test simulating the impact of a tsunami wave on a light-frame timber wall. This model was created because there are multiple data sets from the laboratory tests that could be used to calibrate model parameters so that wave velocities, wave heights, wall reaction forces, and wall deformations are simulated accurately.

The second FE model consisted of a segment of an I-10 bridge over Escambia Bay that was heavily damaged during hurricane Katrina. This causeway bridge was selected, because it is representative of bridge structures in the Gulf region and because datasets exist from past laboratory flume tests that can be used to evaluate the accuracy of the model.

The implementation task will consist of using the computer model of the bridge developed in this project to create a simple guide for practicing professionals and state DOT engineers. The guide and model can be used to identify combinations of storm surge and wave configurations

representative of the Texas-Louisiana Coast, where hydrodynamic forces present the highest hazard to bridge structures.

IMPLEMENTATION STATEMENT

The implementation task will consist of using the developed computer model developed to create a simple guide for practicing professionals and state DOT engineers identifying combinations of storm surge and wave configurations representative of the Texas-Louisiana Coast. The type of modeling technique and bridge model created in this research project can be used to conduct very broad parametric studies to evaluate the effect of various engineering parameters related to wave characteristics and bridge configuration on the force demands at superstructure supports. The scope of the implementation phase will consist of evaluating a range of wave characteristics that are representative of coastal regions in the Texas-Louisiana Coast on the magnitude of support forces.

1. INTRODUCTION

While the US government through its research funding agencies has made a significant investment to mitigate the risk of earthquakes, the investments to improve resiliency to hurricanes has lagged behind significantly. According to estimates by the National Oceanic and Atmospheric Administration (NOAA) the annualized cost of hurricane damage in the US is approximately $10 billion per year; in comparison the Federal Emergency Management Agency (FEMA) estimates earthquake damage to be approximately half that amount. This study addresses that research gap by developing new methods to study the risk to the transportation network from extreme weather events in one of the most important regions in the country in terms of population, economic activity, and transportation systems.

Disruptive weather events in the Gulf Coast and Texas Triangle megaregions (Figure 1) represent a significant risk to the US economy. These two megaregions are of key strategic importance to the mobility of people and goods because they encompass a dense network of large population centers, manufacturing and industrial facilities, military posts, energy processing and distribution networks, and key entry points into the country. Demand on the transportation networks in this area will be exacerbated by projections of population increases as large as 50% over the next 50 years in already highly-populated cities like Houston, San Antonio, and Austin (circles in Figure 1 are indicative of metropolitan area population, i.e. approximately 6.3 million for Houston and 1.3 million for New Orleans). Economic activity, largely concentrated in the Texas Triangle, is among the largest in the US. In the second quarter of 2015 the GDP of Texas was the second largest in the country and represented approximately 10% of the US GDP. Due to the projected growth in population *(2)* and economic activity, studies show that the I-35 and I-10 corridors will become some of the most heavily -used freight routes in the country by 2040.

During disruptive weather events, resilient transportation networks will be needed to minimize the effect on the US and local economies, provide evacuation routes for large population centers along the coast, facilitate post-disaster recovery efforts, and restore economic activity. Past storms illustrate the effect of inadequate planning for resilience. Hurricane Katrina caused widespread damage to the transportation infrastructure in the Gulf Coast megaregion (Figure 1), including damage to highways, the loss of many bridge structures, damage to ports and rail facilities, and waterways. Damage to the port of New Orleans severely affected grain exports and other commodities, impacting freight rates and fuel pricing in the US *(3)*. Damage to the highway system and railways severely impacted the movement of freight through trucks and rail, with Norfolk Southern, CSX, BNSF, and Union Pacific all stopping freight traffic in the New Orleans region in the hurricane's aftermath. Beyond Traffic 2045 *(4)* reports that there are 60,000 miles of coastal roads in low lying areas of the US that are exposed to flooding from heavy rain and storm surge. The damage experienced during Hurricane Katrina highlights the importance of developing a better understanding the risk of large hurricanes and floods to coastal transportation infrastructure. Bridges are a critical component of the transportation network because severe damage and collapse disrupt both emergency response and recovery efforts, and cause very large direct and indirect losses.

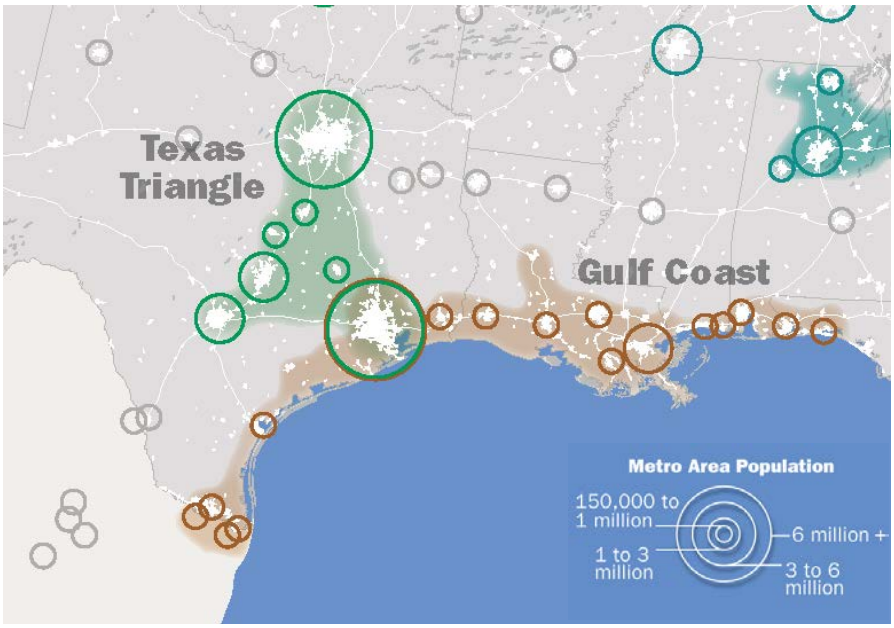

Figure 1. Texas Triangle and Gulf Coast transportation megaregions *(6)*.

Padgett et al. *(5)* indicated the cost of repairing and replacing bridges damaged during hurricane Katrina exceeded $1 billion. Based on a review of inspection reports from state departments of transportation (DOTs), they showed that the most severe damage consisted of superstructure collapse due to unseating of the deck, caused by the combined actions of storm surge and hydrodynamic forces from waves. This type of failure was observed both in bridges with integral and non-integral supports (Figure 2), which shows that in some instances uplift forces were large enough to exceed the weight of the superstructure and cause the failure of the connection at the support. In their review of damage reports, they also found instances in which shear keys were sufficient to prevent unseating of the superstructure at locations where bridges without vertical connectivity nor shear keys suffered collapse of the superstructure. Studies like those by Padgett et al. *(5)* provide a valuable source of information to study the risk to bridge infrastructure due to hurricanes. While documenting damage is important, and some of the empirical observations are useful, there is a need to develop models capable of simulating fluid-structure interaction under the combined actions of storm surge and waves, so the risk can be quantified through a scientific, rather than empirical, approach.

The analysis of bridge structures under wave impact is a very complex problem which involves fluid-structure interaction, where flows become highly nonlinear as they interact with the bridge structure, and the structure develops a dynamic response that affects the loads imposed by the flows around the bridge. Current formulations to calculate forces due to wave impact on bridge structures stem primarily from studies originally developed for off-shore platforms *(1)*. This constitutes an inherent limitation because both the response of the fluid and the dynamic response of the bridge have significant differences with respect to off-shore platforms. Furthermore, owing to the complexity of the problem, most computational models used to study the problem rely on sequential analysis, where water pressures are calculated based on the assumption of a rigid structure, and imposed as quasi-static loads to a flexible structure *(1)*. Physical tests performed with reduced-scale models in flumes are helpful, but limited in their ability to simulate fluid-

structure interaction because the size of flumes limits the scale reduction factor for the structure, and size effects are introduced due to differences in scaling laws of fluids and structures. Furthermore, it is cost-prohibitive to create models that include both bridge substructure and superstructure, so researchers are constrained to use indirect models to simulate the effect of the flexibility of the substructure *(1)*. This study takes advantage of recently-developed multi-physics computational mechanics methodologies to perform fully coupled fluid-structure interaction analyses of bridge structures under wave impact, with the goal of identifying parameters that affect superstructure connection forces using realistic bridge models. The ulterior goal of the models developed in this study is to create a tool that can be used to evaluate bridge response for a range of hydrodynamic load conditions representative of the Texas Louisiana Gulf Coast. These simulations can be used to evaluate current design methodologies to identify discrepancies and knowledge gaps that must be addressed to improve the resilience of bridge infrastructure.

Figure 2. Damage to bridge supports during hurricane Katrina *(4)*.

Because this problem is very complex and inherently multi-disciplinary, information available to engineers tasked with bridge design in coastal regions is limited. Furthermore, procedures referenced in the AASHTO LRFD Bridge Design Specification *(7)* were not developed specifically for bridge structures. This causes a lack of clear understanding on how to proportion superstructure/substructure connections to make bridges resilient to damage from large storms and floods. The AASHTO LRFD Specification describes Water Loads in Section 3.7., which provides equations to calculate pressure of flowing water acting on substructures, is silent on superstructure loads, listing only drag coefficients for different pier shapes. Wave loads are addressed in Subsection 3.7.4, through a broad statement indicating that wave action shall be considered. The commentary of Subsection 3.7.4 directs the user to the latest edition of the Shore Protection Manual published by the Department of the Army *(7)*, which provides formulations for wave pressure based on simplified wave theories that were not developed for bridge superstructures.

More recently, AASHTO published guidelines for estimating maximum slamming and quasi-static wave forces for costal bridges *(9)* based on Kaplan's equations of wave forces on platform deck structures, originally developed for oil platforms *(1)*. These equations were calibrated based on a reduced scale model of the I-10 bridge over Escambia Bay that collapsed during hurricane Ivan *(1, 8)*. The scale of the experiments, the limited range of wave forms, and the fact the models did not include the flexibility of the foundation pose concerns in terms of the validity of the equations that can be evaluated with the models developed in this study *(1)*.

2. OBJECTIVE

The main objective of this study is to develop a high-resolution finite element (FE) model capable of simulating the response of bridge structures to hydrodynamic loads for hurricane design conditions (i.e., surge height, wave height, and frequency) expected in the Texas-Louisiana coast. The significance of the research is that it incorporated a new generation of methodologies for fluid-structure interaction that allow the analysis of the coupled fluid-structure response during wave impact. Models like this will permit the calculation of hydrodynamic forces including the effects of foundation flexibility, which has been shown to have a significant effect on the magnitude of the demands. This model was calibrated using data from physical tests and past hurricanes such as Katrina, and used to evaluate the vulnerability of bridge structures to wave impact.

3. SCOPE

This research focuses on transportation infrastructure, one of the core interdependent systems needed for evacuation, to facilitate disaster response, and a system that is critical during disaster recovery. The scope of the study consists of developing high-resolution FE models to simulate the effect of hydrodynamic forces due to wave impact on bridge structures, accounting for the effects of fluid-structure interaction. These types of models are critical to learn the probability of damage to bridges caused by different types of waves and storm surge.

Several models were developed, with different levels of complexity. The simplest models consisted of wave impacting a bridge pier and bridge girders, and were created with the goal of developing confidence on the simulation of waves, the proper definition of boundary conditions, and the solid-fluid interaction during wave impact. Typical execution time for these models in a high-performance cluster with 24 cores was approximately 2 days per simulation.

Two larger FE models were developed to validate the method of analysis using experimental results from flume tests. These models had a much higher computational cost, with typical execution time in a high-performance cluster with 24 cores of approximately 10 days per simulation. The first of the large models replicated a flume test simulating the impact of a tsunami wave on a timber wall. This model was created, because there are multiple data sets from the laboratory tests that can be used to calibrate model parameters so that wave velocities, wave heights, wall reaction forces, and wall deformations are simulated accurately.

The second large model consisted of a segment of an I-10 bridge over Escambia Bay that was heavily damaged during hurricane Katrina. This causeway bridge was selected, because it is representative of bridge structures in the Gulf coast region and because existing datasets from laboratory flume tests are available that can be used to evaluate the model's accuracy. The model was subjected to impacts from a wave with values of storm surge, wave length, and wave height representative of those expected in the Gulf coast during hurricanes to evaluate the likelihood of bridge superstructure unseating. This second model was used to perform a parametric study to evaluate the effect of substructure flexibility and wave velocity on connection forces between the substructure and the superstructure.

The models created in this study constitute an important step towards more complex studies that evaluate the probability of achieving different damage levels in bridge structures during large storms and hurricanes. The development of fragility relationships for damage levels is not within the scope of this study, but it is the ulterior goal and will be the subject of future research.

4. METHODOLOGY

There are multiple approaches and modeling techniques that can be used for studying wave impact on bridge structures. This is a problem with significant complexity, because fluid and solid behavior are governed by different systems of equations and integrating the two into a single platform that accurately simulates the interaction between them is challenging. For this reason, many past studies have investigated the behavior of the two separately: attempting to calculate the magnitude of the forces imposed by the fluid on the solid and approaching the structural forces as a mechanics of solids problem. The main limitation of this approach is that the interaction between fluid and solid is not properly simulated, because the methodology is not capable of simulating changes in fluid pressures and flow caused by deformations in the structure. Flume experiments by Bradner et al. *(1)* have shown that the coupling between the structural and fluid response can have a significant effect on the magnitude of the hydrodynamic forces calculated through analysis and experimentation. Recent advances in computational mechanics have led to a new generation of methodologies that allow simulating the coupled response of fluid and structure within a single computational platform, which eliminates most of the limitations of past research approaches. A literature review was performed to identify different methods and computational platforms used to study wave impact problems in the past in order to choose a suitable approach for this study.

4.1. Literature Review

The amount of damage incurred during hurricanes like Katrina *(5)* and Ivan *(1)*, and during recent flash flood events in Austin and San Marcos, TX, suggest that wave and flood forces were not adequately considered in the design of the affected bridge structures. Part of the problem stems from the fact that previous research associated with wave forces stems from research on offshore platforms and flat plates *(1)*, which may not be suitable for bridge superstructures due to differences in geometry, profile, and width-to-wavelength ratio *(1)*. Flume experiments used to validate these design procedures were performed using models with very small scales, as low as 1:25, which may have significant size effects associated with Froude scaling *(1)*. Bradner points out that most flume tests were performed with monochromatic waves with equivalent scaled periods exceeding 10 seconds, much higher than wave periods expected in the shallow waters of the bays along the Gulf Coast *(1)*. More recent flume tests used to develop the AASHTO guidelines for the design of coastal bridges *(9)* and the study by Bradner *(1)* relied on models with scale factors of 1:8 and 1:5, respectively. Some of these models did not account for substructure flexibility and some did through the use of elastic springs with various flexibilities *(1)*.

The methodology employed in this study relies on computational mechanics to overcome the limitations of reduced-scale flume tests. A literature review was performed to identify computational mechanic studies on fluid-structure interaction that relied on methodologies suitable for this study or investigated wave impact on bridge structures specifically. A list of references with a brief description of the specific fluid-structure interaction problem of each study and the computational approach used are summarized in Tables 1 – 5. Among the technical references gathered, two different types of general approaches were found. In the first approach, different fluid-dynamics and structural mechanics computational platforms were used, with the fluid-structure interaction problem being solved uncoupled and sequentially. The fluid-dynamics software was used to calculate hydrodynamic pressures or forces that are subsequently applied to the structure in a structural mechanics software platform. The second general approach consisted of evaluating fluid-structure interaction in a single software platform, capable of simulating both

the behavior of the fluid and the solid in two different domains, with the ability to solve the fluid dynamics and structural mechanics problems as a coupled set of equations. Within this second approach two different techniques were identified, Coupled Eulerian-Lagrangian (CEL) techniques and Smooth Particle Hydrodynamics (SPH).

Some of the software platforms identified in the literature have several applications that may be used to study fluid-structure interaction problems. For example, the computer software ABAQUS has CEL, AQUA (a routine used to apply steady current, wave, and wind loading to submerged or partially submerged structures that is used primarily in problems such as the modeling of offshore piping installations or the analysis of marine risers), CFD (an integrated Computational Fluid Dynamics solver to calculate pressure distributions in flow systems for structural analysis), and SPH (a modeling technique in which matter in motion is simulated as a collection of particles).

Other software platforms used by researchers include ANSYS, FLOW-3D, LSDYNA, STAR-CCM+, OPEN-FOAM, WLS (wave load software), and GPUSPH (Weakly-Compressible Smoothed Particle Hydrodynamics, WCSPH, to run entirely on GPU with CUDA). These platforms include structural analysis software, fluid dynamics software, and integrated platforms that offer coupled solution of fluid and structure equations using CEL, CFD, and SPH.

Tables 1 – 5 list examples of fluid-structure interaction problems related to wave impact on bridges with a brief description of the objectives of the research study and the corresponding software platform employed by the researchers.

Studies in Table 1 *(10–15)* relied on a single computational approach in the computer platform ABAQUS. As can be observed in Table 1, the two approaches capable of simulating the coupled response of solid and fluid within ABAQUS are computational fluid dynamics (CFL) and Coupled Eulerian-Lagrangian. Studies by Almasri and Moqbel *(10)* and Sato and Kobayashi *(13)* focused on flow around bridge substructure elements, while the study by Como and Mahmud *(12)* investigated the effect of tsunami waves and debris on coastal structures. Of particular interests to this research is the study by Do et al. *(11)* who performed simulations of wave impact on bridge superstructures to generate fragility relationships. This study was used as a reference for the models developed in this study.

Studies summarized in Table 2 *(16–21)* relied on a combination of software platforms to perform sequential analysis. A first stage simulated the response of the fluid with a rigid structure and calculated water pressures imposed on a structural model developed in ABAQUS. Examples of software platforms used to analyze the fluid dynamics component includes STAR-CCM+, widely used in the automotive and aerospace industries, and the wave load software, a set of software routines that generates wave-based surface and body forces due to buoyancy, drag, and inertial effects. The majority of these studies focused on the effect of substructure shape on the drag coefficient for bridge substructure elements. The study by Gullet et al. *(18)*, is of greatest significance to this study because it focused on damage due to unseating of bridge superstructures. They concluded that guidance for wave loading on bridges is less mature than that for wave loading for offshore platforms, and that further research is needed in regards to wave loading due to storm surge. They also found that the computational simulations did not fully capture the vertical loads measured in flume tests when typical inertia and drag coefficients were used. The finite element

model by Gullet et al. did not account for the effect of foundation flexibility on fluid-structure interaction. Bozorgnia, et al. *(21)* also studied the effect of buoyancy forces, which were shows by damage reports to have played a very important role on superstructure collapses during hurricanes Katrina and Ivan *(1)*.

The study by Istrati and Buckle listed in Table 3 used advanced fluid-structure interaction analyses in LS-DYNA and showed that superstructure and substructure flexibility significantly influenced the magnitude of calculated bridge and connection forces due to tsunami wave impact. They also concluded that superstructure and substructure flexibility affected the distribution of fluid forces, which changed the dynamic response of the bridge.

The study by Briker et al. in Table 4 *(31)* was motivated by the large number of bridge failures that occurred in the Miyagi and Iwate Prefectures during the Tsunami caused by the Great East Japan Earthquake. Briker et al. used OpenFOAM, an open source C++ toolbox with computational dynamics capabilities, to create a two-dimensional model of a typical bridge superstructure. They found that deck inclination, flow speed, trapped air, entrained sediment, and tsunami surge were the primary factors contributing to bridge superstructure failure. They studied two different scenarios, one in which the bridge is impacted by sloping water surging into the structure suddenly by tsunami surge, representative of conditions in the southern Miyagi Prefecture, and a case where the bridge is engulfed by a smoothly rising water surface, representative of conditions in the Utatsu Prefecture. For steady flow scenarios they found that entrapped air posed the greatest threat to the bridge structure, while in the case of water surge the overturning moment was of greatest concern.

Studies in Table 5 *(37–41)* employed the SPH methodology for a variety of fluid-structure interaction problems including impact of tsunami bore on bridge piers *(38)*. In these studies, the SPH methodology was successfully implemented to simulate impact problems, and is particularly useful where there is fragmentation after impact or highly nonlinear flow.

Because one of the goals of this study was to take advantage of newly developed software that integrates fluid and solid in a single platform, two different approaches were selected as potential methodologies to be used in this study: CEL and SPH. Co-simulation of the fluid and structural response in the same platform allows a realistic representation of bridge response that overcomes significant limitations of past methodologies. Using CEL and SPH it is possible to create models that include the bridge structure, substructure (potentially including the foundation as well), and the fluid, where fluid pressures and fluid velocities change in response to the dynamic response of the bridge. Both of these methodologies are capable of simulating highly nonlinear flows that originate near complex solid shapes such as prestressed bridge *I* girders. Also, both of these platforms allow the simulation of a wide range of wave configurations, including monochromatic and random waves.

A brief description of the CEL and SPH methodologies is presented in Section 4.2.

Table 1. Related fluid-structure interaction problems simulated using Abaqus.

Author	Year	Title	Description	Method
Almasri and Moqbel *(10)*	2017	Drag Force Coefficients of Water Flow Around Bridge Piers	Investigates the drag coefficient of flow around square, semicircular-nosed, and 90^{o} wedged-nosed and circular piers	Computational Fluid Dynamics (CFD) Navier–Stokes equation
Do et al. *(11)*	2016	Performance-based design methodology for inundated elevated coastal structures subjected to wave load	Compute forces on elevated coastal structures	Combined Eulerian–Lagrangian (CEL)
Como and Mahmound *(12)*	2013	Numerical evaluation of tsunami debris impact loading on wooden structural walls	Study impact of debris on interior and exterior wood structural panels	Coupled Eulerian–Lagrangian (CEL)-(CFD)
Sato and Kobayashi *(13)*	2012	A fundamental study of the flow past a circular cylinder using Abaqus/CFD	Fluid flow around a circular cylinder placed in a uniform flow was investigated focusing on the occurrence of various phenomena associated with von Karman vortices and the oscillation of a circular cylinder excited by these vortices over the object.	Computational Fluid Dynamics (CFD)
Smojver and Ivančević *(14)*	2011	Bird strike damage analysis in aircraft structures using ABAQUS/Explicit and coupled Eulerian Lagrangian approach	Damage prediction procedure and damage assessment of bird impact on a typical large airliner inboard flap structure	Coupled Eulerian–Lagrangian (CEL)
Bai et al. *(15)*	2008	Seismic Response Analysis of The Large Bridge Pier Supported by Group Pile Foundation Considering the Effect Of Wave And Current Action	Study of a bridge system including the pier-pile-soil system. Pile seismic response characteristics in the lenitic condition, including the influence of wave and current actions, were analyzed. The influence of wave height and current velocity on pile seismic response was discussed.	Morison's hydrodynamic pressure formula/Stokes fifth-order wave theory viscous-plastic memorial nested the yield surface

Table 2. Related fluid-structure interaction problems simulated using Abaqus + STAR-CCM+ / WLS.

Author	Year	Title	Description	Method
Chiarelli et al. *(16)*	2013	Fluid-Structure Interaction Analyses of Wings with Curved Planform: Preliminary Aeroelastic Results	Study of wave drag effects on two half-wing models, having curved and swept planform.	Star-CCM+® 6.04.14 and ABAQUS
Chiarelli et al. *(17)*	2013	The Effects of Platform Shape on Drag Polar Curves of Wings: Fluid-structure Interaction Analyses Results	Study on how to compute forces on elevated coastal structures.	Combined Eulerian–Lagrangian (CEL)
Gullett et al. *(18)*	2012	Numerical Modeling of Bridges Subjected to Storm Surge for Mitigation of Hurricane Damage	Study of forces on highway bridges as a result of storm surge and wave action, and use these forces to investigate the feasibility of rapid retrofit techniques to prevent failure	ABAQUS+WLS (wave load software)
Bozorgnia and Lee *(19)*	2012	Computational Fluid Dynamic Analysis of Highway Bridges Exposed to Hurricane Waves	Two-phase Navier Stokes equations were used to evaluate hydrodynamic forces exerted on prototype of I10 Bridge	Navier Stokes type /hydrodynamic forces Star-CCM+
Sewell *(20)*	2012	Wave Loads on Multi-member Offshore Wind Turbine Sub-structures	Evaluate hydrostatic and hydro-dynamic loads on two multi-member offshore wind turbine substructures, a jacket, and a tripod, and compare the results to common modeling methods of predicting wave loads based on Morison's equation	Reynolds-averaged Navier-Stokes (RANS) equations Star-CCM+
Bozorgnia, et al. *(21)*	2011	Wave Structure Interaction: Role of Entrapped Air on Wave Impacts and Uplift Forces	Investigate the role of entrapped air on hydrodynamic forces exerted on bridge superstructure	Navier Stokes type /hydrodynamic forces Star-CCM+

Table 3. Related fluid-structure interaction problems simulated using Flow-3D / LS-DYNA.

Author	Year	Title	Description	Method
Erduran et al. *(22)*	2012	3D Numerical Modelling of Flow Around Skewed Bridge Crossing	Calculation of water surface profiles using a series of experimental data obtained in a two-stage channel with skewed bridge crossing.	Flow-3D
Lau et al. *(23)*	2011	Experimental and Numerical Modeling of Tsunami Force on Bridge Decks	Simulate tsunami flow around I-girder bridge	Flow-3D
Kocama et al. *(24)*	2010	3D model for prediction of flow profiles around bridges	Solve the Reynolds averaged Navier–Stokes equations, to predict the free surface profiles from up- to downstream of four different bridge types with and without piers in a compound channel	Flow-3D
Zong et al. *(25)*	2016	Collapse Failure of Prestressed Concrete Continuous Rigid-Frame Bridge under Strong Earthquake Excitation: Testing and Simulation	Two-phase Navier Stokes equations are used to evaluate hydrodynamic forces exerted on prototype of I10 Bridge	LS-DYNA
Istrati et al. *(26)*	2017	Tsunami Induced Forces in Bridges: Large-scale Experiments and The Role of Air-entrapment	Large scale hydraulic experiments of tsunami waves impacting a straight composite I-girder bridge	LS-DYNA
Azadbakht and Yim *(27)*	2015	Estimation of Cascadia Local Tsunami Loads on Pacific Northwest Bridge Superstructures	A comparison between tsunami loads on a deck-girder bridge and a box-girder bridge under identical tsunami flow condition.	LS-DYNA
Istrati and Buckle *(28)*	2014	Effect of Fluid-structure Interaction on Connection Forces in Bridges Due to Tsunami Loads	Study to determine tsunami forces on bridge connections.	LS-DYNA

Table 4. Related fluid-structure interaction problems simulated using Flow-3D / LS-DYNA.

Author	Year	Title	Description	Method
Shahbaboli *(29)*	2016	Numerical Modeling of Extreme Flow Impacts on Structures	The dam-break approach is used to investigate the tsunami-like bore interaction with structures	OpenFOAM
Chen et al. *(30)*	2014	Numerical investigation of wave–structure interaction using OpenFOAM	Study non-linear wave interactions with offshore structures for a range of wave configurations.	OpenFOAM
Bricker et al. *(31)*	2012	CFD Analysis of Bridge Deck Failure Due to Tsunami	OpenFOAM computational fluid dynamics package was used to determine the effects of lift, drag, and moment on a typical bridge deck based on two-dimensional Reynolds-averaged simulations.	OpenFOAM
Xu and Cai *(32)*	2017	Numerical investigation of the lateral restraining stiffness effect on the bridge deck-wave interaction under Stokes waves	Study to evaluate if bridge deck vibrations result in smaller wave forces on the deck.	ANSYS
Zhang et al. *(33)*	2015	Optimum Design of Bridge Cross Section with Low Clearance Considering Wave Load Effects Based on Numerical Wave-Tank	Numerical simulation results of wave forces acting on three kinds of twin-deck girders (circular arc box girder, trapezoid box girder and T-shaped girder) of bridge with low clearance crossing sea.	ANSYS
Xu and Cai *(34)*	2015	Numerical simulations of lateral restraining stiffness effect on bridge deck–wave interaction under solitary waves	Seismic response of fabricated box girder bridge considering the traveling wave effect based on ANSYS	ANSYS
Qian-hui and Zheng-xin *(35)*	2014	Traveling Wave Effect Analysis on Fabricated Box Girder Bridge Based on ANSYS	Seismic response of fabricated box girder bridge considering the traveling wave effect based on ANSYS	ANSYS
Debus et al. *(36)*	2003	Computational Fluid Dynamics Model for Tacoma Narrows Bridge Upgrade Project	Validate and apply a commercial computational fluid dynamics code with a hybrid RANS/LES turbulence computational model	ANSYS

Table 5. Fluid-structure interaction problems simulated using SPH.

Author	Year	Title	Description	Method
Shadloo et al. *(37)*	2016	Smoothed particle hydrodynamics method for fluid flows, towards industrial applications: Motivations, current state, and challenges	Summarizes reasons for utilizing the SPH method in an industrial context, and describes a state-of-the-art of present applications of this method to industrial problems	SPH
Wei et al. *(38)*	2015	SPH modeling of dynamic impact of tsunami bore on bridge piers	Simulation of a well-conducted physical experiment on a tsunami bore impingement on vertical columns with an SPH model, GPUSPH	GPUSPH
Zhang et al. *(39)*	2013	Numerical simulation of column charge underwater explosion based on SPH and BEM combination	SPH numerical model was combined with Boundary Element Method (BEM) to simulate the whole process of underwater explosion detonated by column charge	SPH-BEM
Liu et al. *(40)*	2003	Smoothed particle hydrodynamics for numerical simulation of underwater explosion	A meshless, Lagrangian particle method, smoothed particle hydrodynamics (SPH), is applied to simulate underwater explosion problems	Lagrangian Particle Method with SPH
Liu et al. *(41)*	2002	Investigations into water mitigation using a meshless particle method	Studies water mitigation problems by using smoothed particle hydrodynamics (SPH), which is a meshless, Lagrangian method well-suited for large deformation explosion events with significant homogeneities	Lagrangian Particle Method with SPH

4.2. Modeling Approach

4.2.1. Coupled Eulerian-Lagrangian (CEL) Analysis

This methodology is based on solving simultaneously two coupled systems of equations with different coordinate systems, to calculate deformations in a solid (Lagrangian coordinates) and the motion of a fluid (Eulerian coordinates) (Figure 3).

Lagrangian meshes are attached to material points, and as materials deform, the mesh deforms with them (Figure 3a). Because elements distort as they deform and calculated deformations and stresses become inaccurate in highly distorted meshes, the Lagrangian method is not a good approach for materials subjected to extreme deformations like fluids or highly distorted solids.

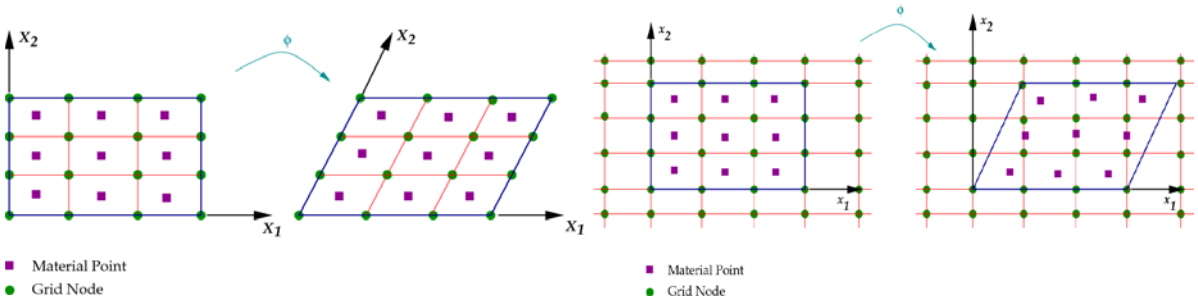

a) Langrangian Mesh b) Eulerian Mesh

Figure 3. Eulerian and Lagrangian meshes.

Eulerian meshes remain the same as the material flows (or deforms) within the mesh (Figure 3b). The extent of deformation in this case is measured when the material particle flows across an element node (it acts as a background grid). Eulerian meshes are formulated to track the motion (velocity) of fluids through fixed location points so the mesh remains undeformed as the material flows within the mesh. Because the accuracy of this approach is not affected by magnitude of the deformations this method is best suited for materials that undergo extreme deformations like fluids. This methodology has been implemented in commercially available finite element software like ABAQUS and LS DYNA, and has the significant advantage that the behavior of fluids and solids can be simulated under a single software platform. A sample simulation of flow around a round pier performed at the early stages of this study is presented in Figure 4. The color pattern in the fluid and the pier represents the magnitude of the displacements.

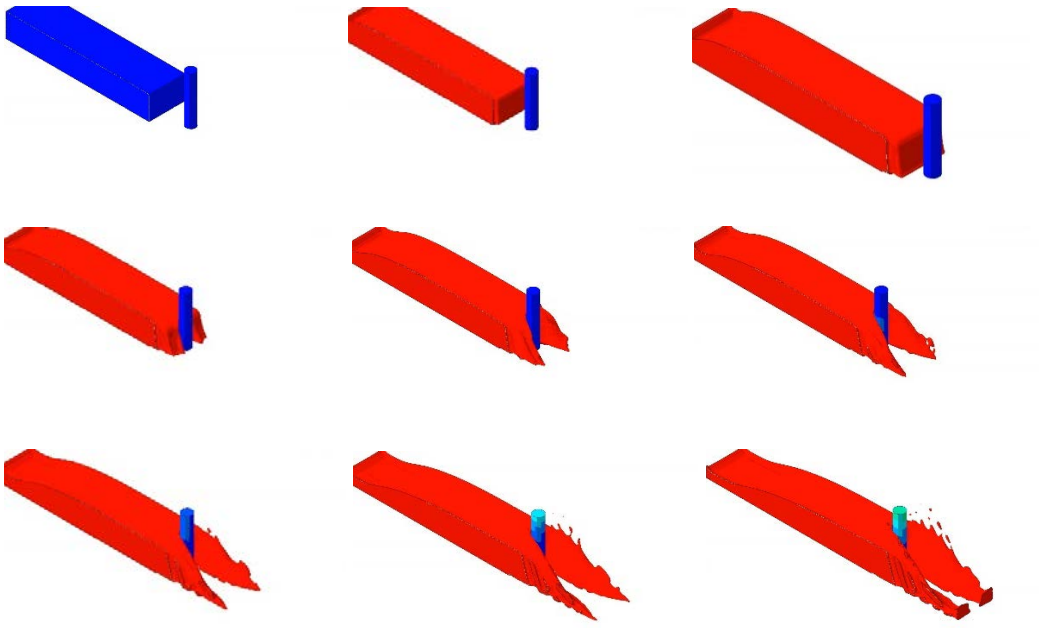

Figure 4. Coupled Eulerian-Lagrangian simulation of flow around a round pier.

4.2.2. Smoothed Particle Hydrodynamic (SPH) Analysis

SPH is a meshless methodology where the solution of the partial differential equations describing the motion of bulk matter is approximated using macroscopic particles. In the SPH method derivatives of continuum field variables are computed on an irregular grid composed of many moving particles. The novelty of the SPH methodology is that it provides a method for smooth interpolation and differentiation within an irregular grid of moving particles. In this method, the "grid" of particles lacks memory of its initial configuration, which makes it self-healing. An example of fluid flowing between two tanks simulated using SPH is presented in Figure 5. In this particular example, the tanks were modeled using rigid solids and the fluid flows from a full to an empty tank as a gate is lifted.

The technique can be adapted for use in structural dynamic problems by incorporating constitutive equations into SPH, allowing its use to analyze a wide range of problems such as elastic flow, multi-phase flows, shock simulations, mass flows, high (or hyper) velocity impact (HVI) problems (where shock waves propagate through colliding bodies that behave like fluids), impact problems such as explosions generated by the detonation of high explosives (catastrophic wave destruction), underwater explosions, underwater shock, and water mitigation of shocks.

In the context of fluid-structure interaction problems, the SPH technique is an alternative to Eulerian analysis and is used primarily to simulate the behavior of fluids. Similar to Eulerian analysis, this methodology becomes most powerful when it is combined with Lagrangian analysis, because the joint simulation platform allows solving for coupled fluid-solid interaction problems.

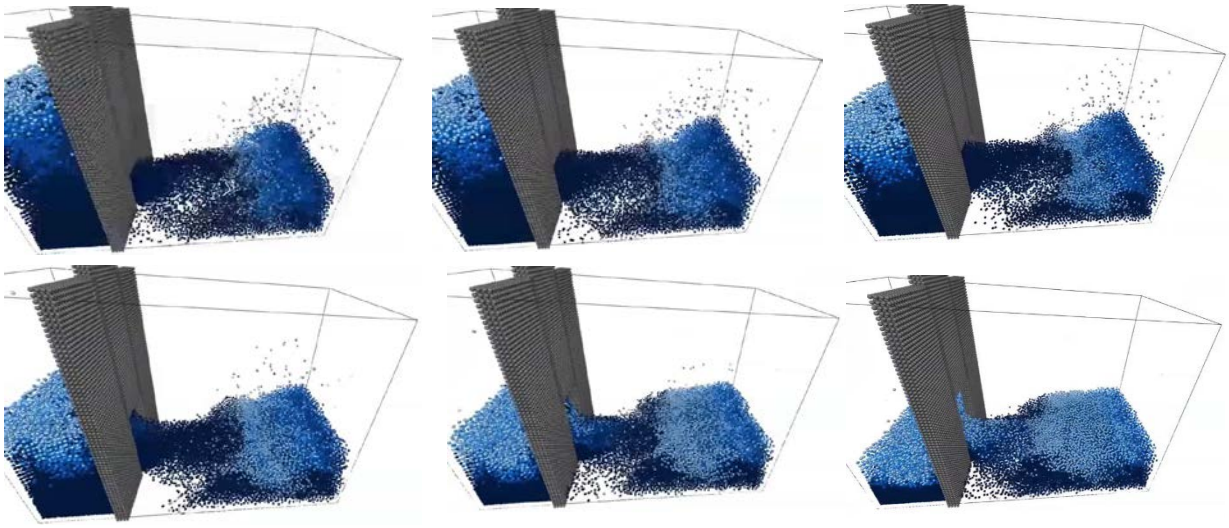

Figure 5. SPH simulation of flow between two tanks.

4.2.3. Modeling Approach Adopted

Consideration was given to both CEL and SPH analysis techniques for the methodology to be used in this study. FE models illustrated in Figures 4 and 5 were created to evaluate the computational cost and feasibility of both techniques to simulate controlled wave forms, flow inlets and outlets, and controlled boundary conditions at the edges of the models. At the present stage of software

development, the CEL platform was found to be better suited for this study, because the computational cost was significantly lower and software implementations of SPH are still in early stages of development in regard to the simulation of boundary conditions. Specifically, for the ABAQUS software, the 2017 version does not permit the simulation of inlet and outlet of flows in SPH analysis, complicating the simulation of the wave impact problem significantly. For these reasons, it was decided that the CEL analysis methodology would be used in this study.

An important consideration in the simulation of wave impact problems, particularly in the case of bridge structures, is the accuracy of the flow in regions surrounding complex solid shapes, such as American Association of State Highway and Transportation Officials (AASHTO) bridge girders. The representation of flow in these regions is highly mesh-sensitive, where the accuracy improves with mesh density. For the purpose of this study, it was important to conduct simulations to define Eulerian mesh densities that would result in accurate representations of flow in areas where waves impacted AASHTO bridge girders, and doing so at a reasonable computational cost. Because the execution time in a high-performance of the complete bridge model was approximately 10 days, mesh studies were performed using smaller FE models, that could be completed within two days. A high-resolution FE model of a wave impacting a single AASHTO girder was created with the purpose of evaluating the effect of mesh density on the representation of flow in the vicinity of the bridge girders during wave impact, and to define minimum acceptable Eulerian mesh densities to be used in the study. The model was created using the computer software ABAQUS with Coupled Eulerian-Lagrangian analysis (CEL), where solids were simulated with Lagrangian meshes and fluids were simulated using Eulerian meshes (Figure 6). Results from sample simulations of the wave impacting an AASHTO bridge girder are shown in Figure 6. The wave was simulated by imposing a sinusoidally-varying initial velocity field on the fluid, at the edge of the Eulerian domain. Variations in wave properties (wavelength and amplitude) were introduced by adjustments in the boundary conditions of the fluid domain. A fluid inlet boundary condition was created on the left edge of the Eulerian domain of the model and an outlet boundary condition on the right edge, so waves would follow a left-to-right motion and not be reflected when reaching the right edge. Figure 6 shows that flow around the bottom of the *I* shape was modeled smoothly for the mesh density used in the model.

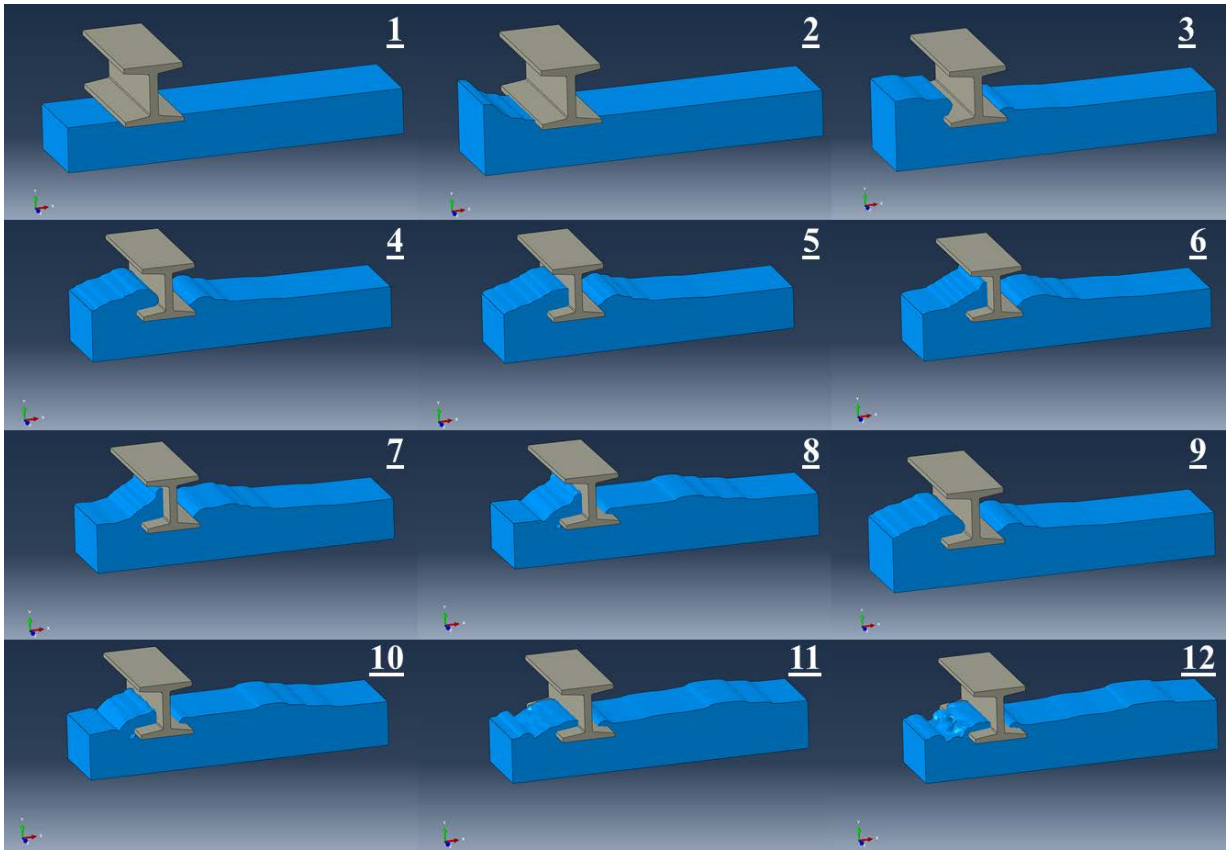

Figure 6. Finite element model of wave impact on AASHTO bridge girder.

The effect of wave impact on the girder stress field is illustrated in Figure 7. This model was created to verify that the interaction between the fluid and the solid resulted in deformations and stress demands within the solid.

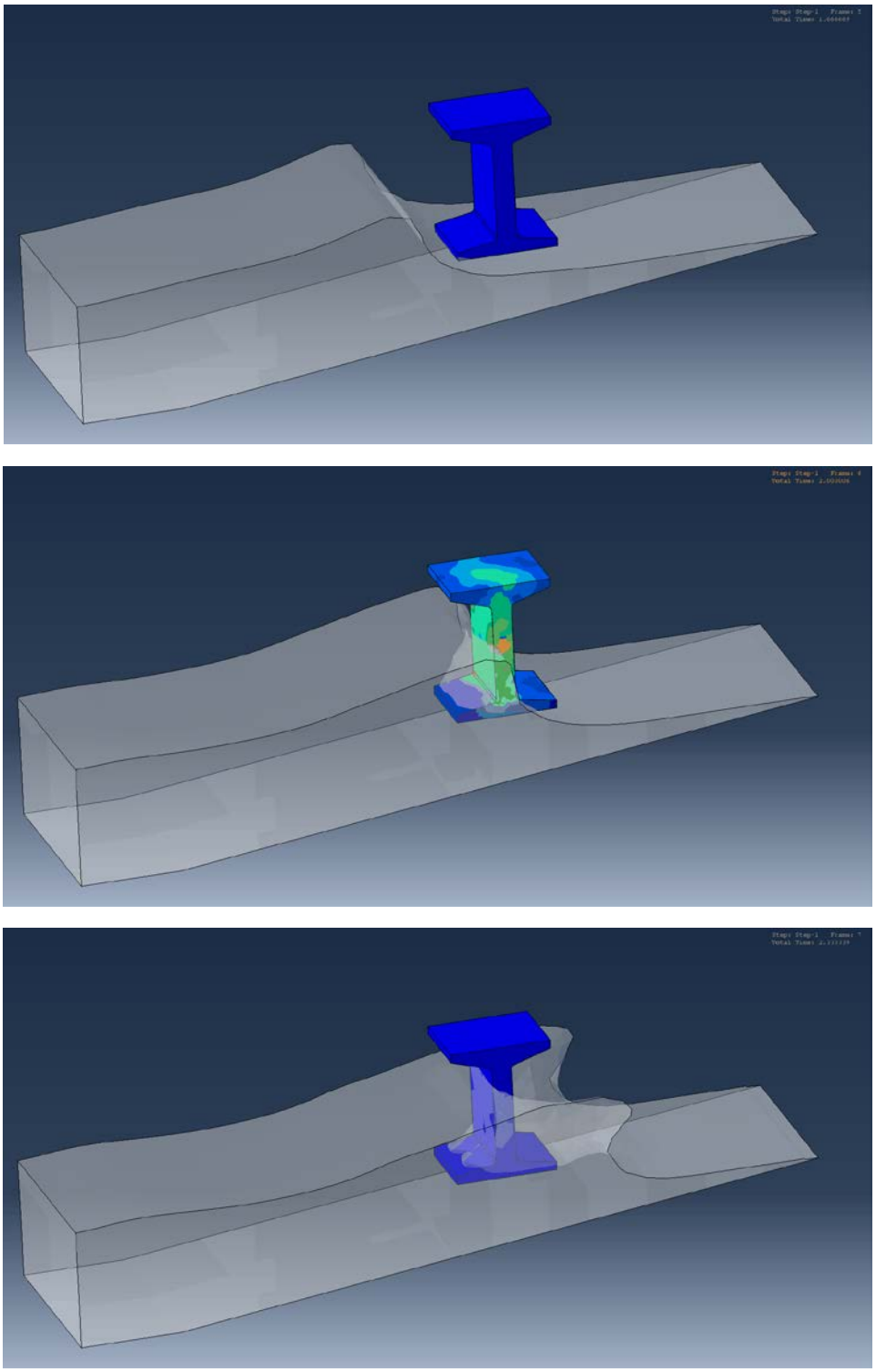

Figure 7. Effect of wave impact on stress field of bridge girder.

4.3. Tsunami Wave Calibration Model

Preliminary simulations described in Section 4.2 were performed with the primary goal of developing confidence on simulation of wave impact and highly nonlinear flow around the complex shape of bridge girders. The next step in the research methodology was to develop an

understanding of how to adjust inlet initial conditions to generate specific wave velocities and amplitudes, and to evaluate if the magnitude of fluid pressures and corresponding reaction forces generated on the solid elements during impact were consistent with experimentally measured values. Tsunami wave experiments performed in test flumes were particularly useful for this purpose because in this type of experiments waves advance without any disruption until they break and impact beach structures. Data sets from tsunami wave experiments allowed tracking the motion of the wave while it was unaffected by interaction with structures, as well as evaluating the magnitude of the forced generated by wave impact on structures. Several experimental tests of this kind have been conducted in the large wave flume at Oregon State University (Figure 8). A calibration model was created using the computer software ABAQUS with CEL analysis. The computer model replicated experiments of a Tsunami wave impacting a light-frame timber wall rigidly supported on the beach. Calculated impact forces were validated by comparing calculated and measured timber wall reaction forces *(43)*. The light-frame wall had 2 × 6 studs with a spacing of 16 in. (40.6 cm). The test flume used in the experiments had a wave maker with a 13.2 ft (4-m) stroke and maximum speed of 13.21 ft/s (4 m/s) with the capability of producing repeatable single waves as well. The flume was 341 ft (104 m) long, 12 ft (3.66 m) wide with a depth of 15 ft (4.57 m). The flat section in front of the wavemaker was 95 ft (29 m) long followed by an impermeable beach with a length of 85 ft (26 m) and a slope of 1:12. The rest of the flume included a flat floor of 24 ft (7.3 m) with a false-height of 8 ft (2.36 m).

Dimensions of the computer and physical models and boundary conditions used in the Abaqus model are presented in Figures 8 and 9. Experimental measurements were recorded at three different locations shown in Figure 8. Location 1 was instrumented to track water elevation, location 2 was instrumented to track water velocity, and location 3 was instrumented to track the deformation of the light-frame wall (Figure 9). Measurements from locations 1 and 2 were used to evaluate the simulation of flow in the Eulerian mesh while deformations recorded at location 3 were used to evaluate the performance of the Lagrangian mesh. Surface interaction was evaluated using the reaction forces recorded with load cells placed at the light-frame wall.

Boundary conditions in the computer model were defined as shown in Figure 9. Velocity in all three main axis directions (i.e., *x, y,* and *z*) at the flume bottom were set to zero (Figure 10) to prevent water from draining out from the domain (replicating the impermeable beach in the test flume). Boundary conditions at side surfaces of the flume were modeled as having zero velocity only in a direction perpendicular to flume sides (z-direction), i.e., water was allowed to move freely along the sides without any disruption. In the numerical model a sinusoidal initial velocity profile at the boundary of the Eulerian domain replaced the wavemaker used in the experiment. To simulate free flow out of the flume, pressure at the end of the domain was set to zero. Water was initially defined in the flume as presented in Figure 11. The interface boundary condition between water and the transverse wooden wall was defined using the general contact definition provided in the ABAQUS software. This type of interaction surface allows water to rise behind the wall without any restriction. Some simplifications were made to reduce computational cost. The light-frame wood wall was modeled as a flat wall with a thickness of 2.5 in. (65 mm) to maintain the stiffness of the wall with 2 × 6 studs and plywood sheathed *(43)*. The modeled wall had dimensions of 7.5 × 21 ft (2.24 × 3.58 m). The length of the first flat zone in front of the wavemaker was reduced to 8 ft (2.5 m) as shown in Figure 9.

Figure 8. Large Wave Flume at Oregon State University *(42)*.

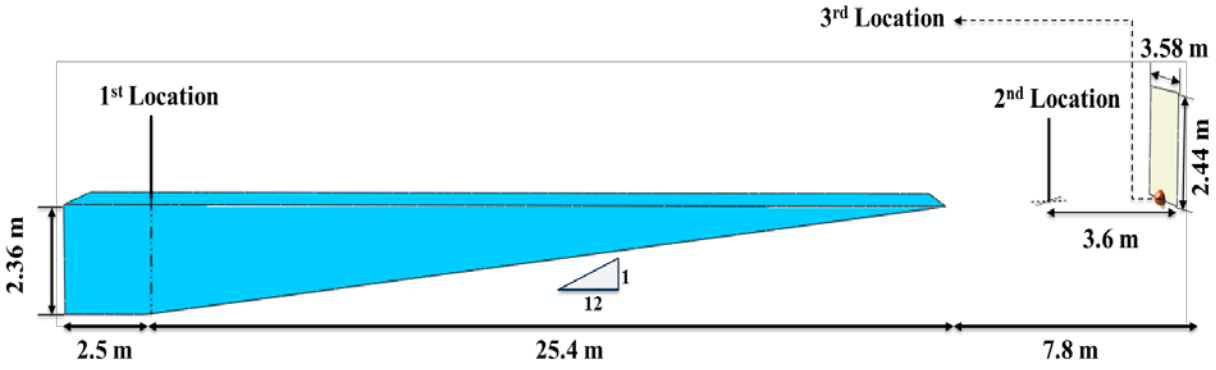

Figure 9. Dimensions of tsunami wave impact calibration model.

There were two material definitions used for the Eulerian domain: water and void (Figure 11). Material properties for water were defined as fluid with U_s-U_p equations of state, specifically with Mie-Grüneisen equations of state and a linear Hugoniot form. Material properties for the Eulerian

fluid are presented in Table 6, and material properties for the Lagrangian solid are presented in Table 7. Interactions between the Lagrangian elements and free material surfaces in the Eulerian domain were defined using the "Frictionless General Contact" in the ABAQUS software. The Eulerian domain was meshed with 8-node linear Eulerian brick elements with reduced integration and hourglass control (EC3D8R). Lagrangian solids in the bridge mesh were modeled using 8-node linear brick, reduced integration, elements with hourglass control (C3D8R).

Table 6. Eulerian material properties for water.

Property	Value
Density	
SI Units (tonne/m^3) [kg/m^3]	1×10^{-9} [1000]
US Units (lb/in^3)	0.03613
Dynamic Viscosity	
SI Units (N s/m^2) [Pa s]	0.001×10^{-4} [0.001]
US Units (lb s/ft^2)	0.000022

Table 7. Lagrangian material properties for concrete.

Property	Value
Density	
SI Units (tonne/m^3) [kg/m^3]	2.4×10^{-6} [2400]
US Units (in. lb)	2.24×10^{-4}
Young's Modulus	
SI Units (MPa) [Pa]	30×10^3 [30×10^9]
US Units (ksi)	4350
Poisson's Ratio	
SI Units	0.2 [0.2]
US Units	0.2

Results from a wave impact FE simulation with an initial wave velocity of 7.3 ft/s (2.2 m/s) are shown in Figure 12. The image sequence shows the progression of the wave through the flume from its origin at the wavemaker in the flat segment of the flume, through the sloped segment, to the time at which it impacts the light-frame wall. The same progression is shown in the sequence of wave elevation profiles presented in Figure 13. The accuracy of the wave simulation at its origin was evaluated using water elevation measurements recorded at location 1 of the flume (Figures 14 and 15). Measured and calculated water elevation at location 1 as a function of time are presented in Figure 15. The close agreement between the FE model and the water elevation in the flat segment of the flume indicate that the velocity profile and boundary conditions used to generate the wave in the FE model provided an accurate representation of the characteristics of the wave for the experimental data set used in the calibration.

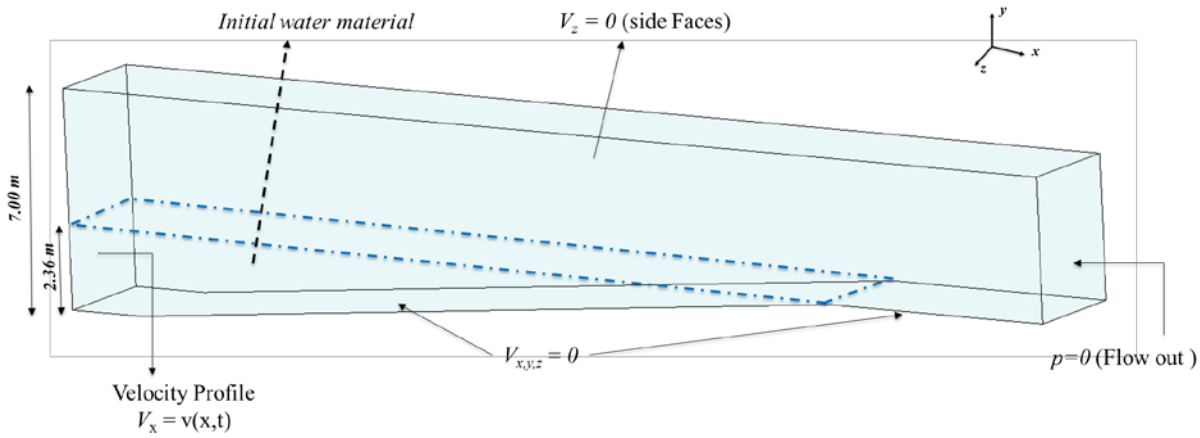

Figure 10. Boundary conditions for tsunami wave impact calibration model.

Figure 11. Material definition in Eulerian Domain.

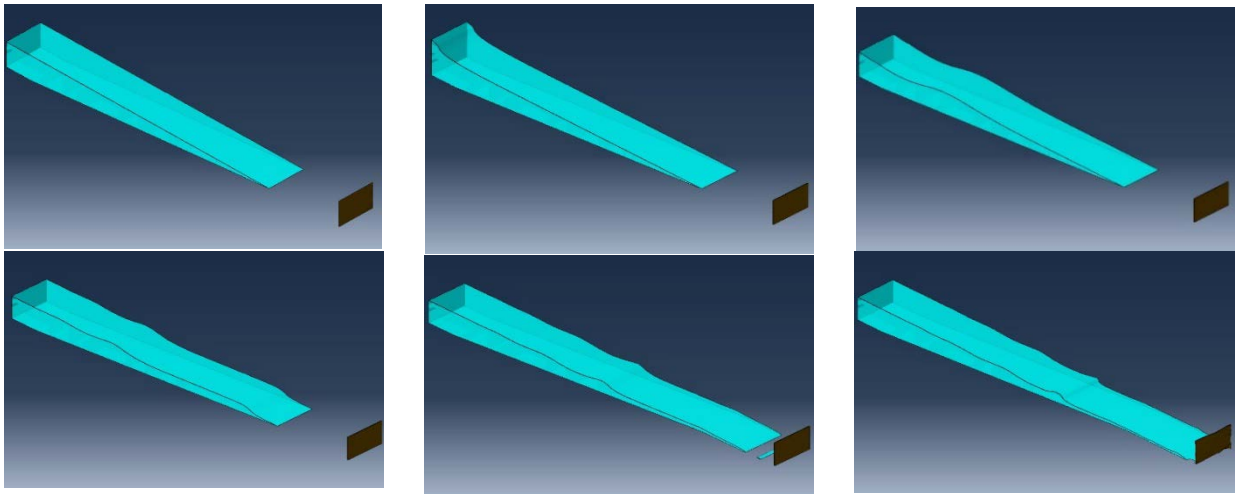

Figure 12. Wave simulation with an initial velocity of 2.2 *m/s*

Figure 12. Elevation profile of tsunami wave traveling towards timber wall.

Water velocity at location 2 (Figures 16 and 17) was monitored to evaluate the accuracy of flow simulation at a point near the wall, in the sloped segment of the flume. Water velocity readings, presented in Figure 17, show asymptotic convergence to measured values. Calculated water velocity values show the effect of the wave as it travels through the location of the sensor. This trend was not reflected by the sensor readings although it is possible that this was due to the highly disrupted nature of the flow caused by breaking of the wave, or by differences between the location where the wave breaks in the computer and physical simulations.

Water elevation and water velocity readings shown in Figures 15 and 17 provide indicators of the accuracy of the Eulerian modeling of water flow in the computer model. Agreement between measured and calculated water elevations and velocities are important to demonstrate that the behavior of the fluid was accurately simulated, to determine fluid material model simulation parameters, and to learn about the relationship between wave characteristics and the initial velocity profile specified at the inlet boundary.

The effect of water velocity profile at the boundary inlet on wave characteristics is illustrated in Figure 18. This figure shows wave elevation profiles at six different times during the simulation for two different initial boundary velocities. The comparison shows that increasing boundary wave velocity lead to an increase in wave amplitude. In the ABAQUS platform, the user can also control the amount of time over which the inlet boundary condition is enforced, so a combination of initial

velocity and boundary enforcement duration provided the means to control wave amplitude and wave length.

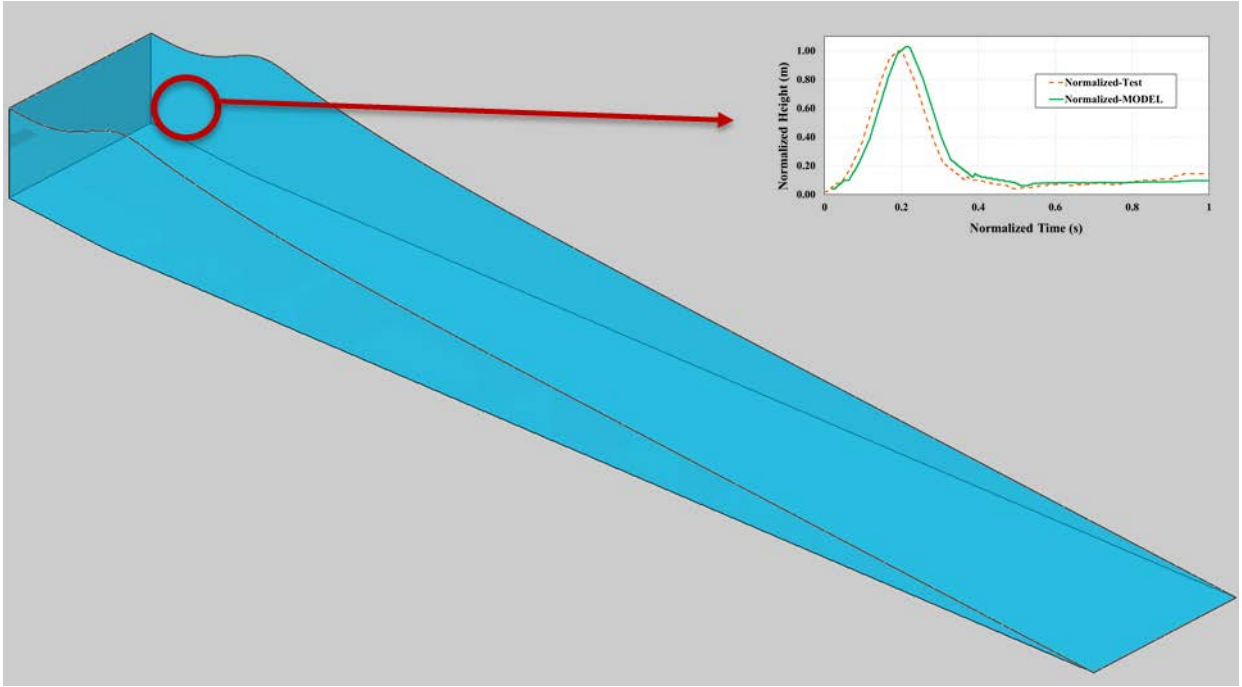

Figure 13. Water elevation at control point 1 of tsunami wave impact model.

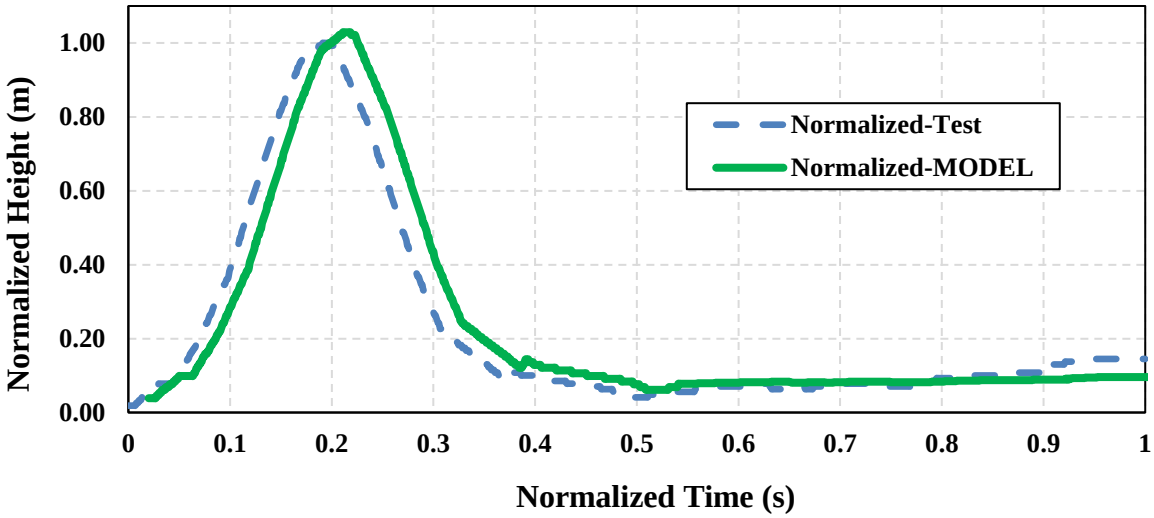

Figure 14. Measured and calculated normalized height at control point 1 of tsunami wave impact model.

Because the objective of the project was to determine the magnitude of the reaction forces at bridge supports, the ability to simulate accurately the interaction between fluid and solid during wave impact is of fundamental importance. A full-length simulation of a high-velocity tsunami wave impacting a light-frame wall is shown in Figure 19. The wave was created through inlet boundary conditions at t_1 and began to break at t_5. The purpose of the comparisons presented in Figures 15 and 17 was to ensure that the simulation was accurate through the entire time the wave traveled

through the flume, between t_1 and t_8. The remaining comparisons presented in this section were intended to ensure that the impact of the wave on the light-frame wall, observed at times t_8 and t_9, yielded accurate estimates of water pressures and wave-induced impact forces on the wall. Two different measurements were used to evaluate the accuracy of wave impact forces on the Lagrangian solid in the tsunamic calibration model. The first was the displacement of the wall at control location 3 (Figure 20). The calculated displacement at wall location point 3, shown in Figure 21, is a function of the magnitude of the water pressure and corresponding wave impact forces, and of the flexibility of the light-frame wall model. Given the uncertainties associated with estimating both of these quantities the accuracy of the calculated displacement was excellent and indicates that the CEL analysis methodology was successful for the purpose of calculating wave impact forces.

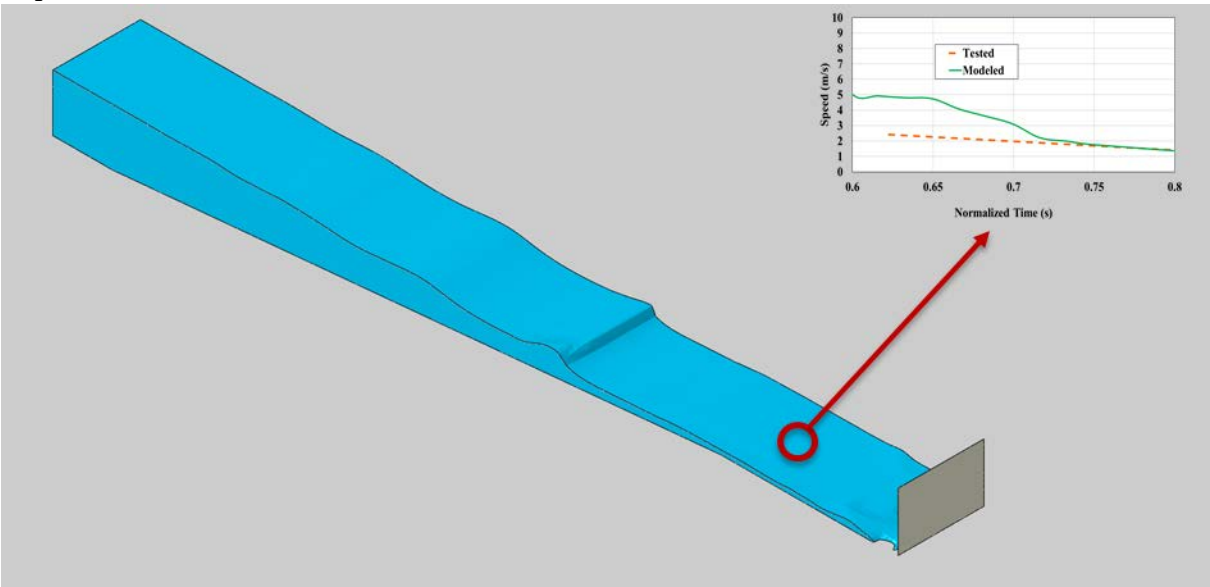

Figure 15. Water elevation at control point 2 of tsunami wave impact model.

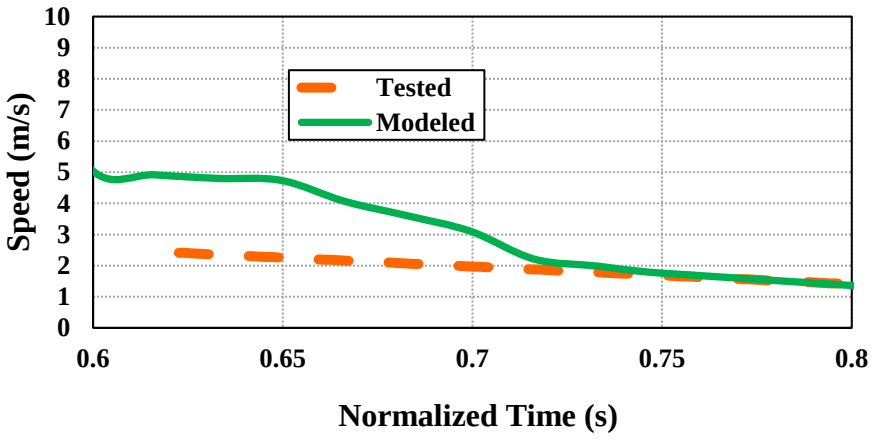

Figure 16. Measured and calculated water speed at control point 2 of tsunami wave impact model.

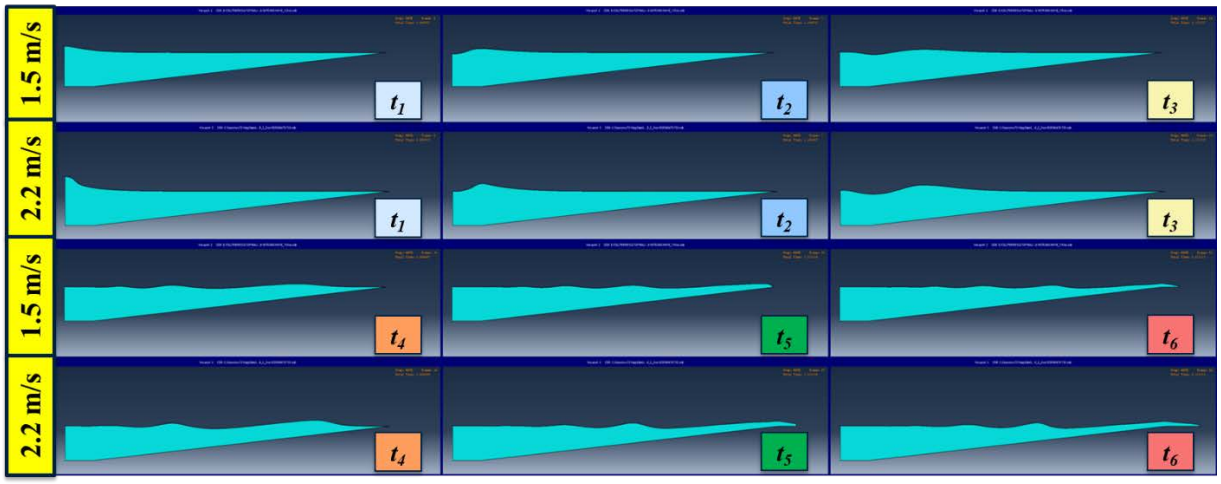

Figure 17. Comparison between wave profiles with initial velocities of 1.5 m/s and 2.2 m/s.

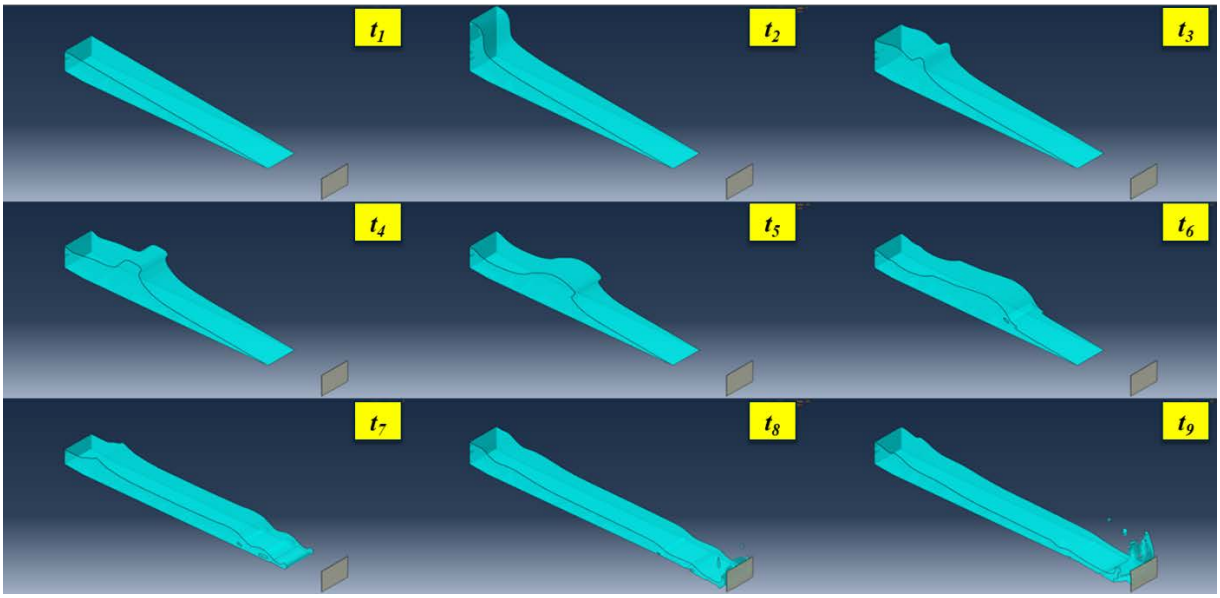

Figure 18. Tsunami wave impact simulation sequence for high velocity wave.

A comparison between measured and calculated reaction forces at wall supports due to wave impact provides a more important measure of the accuracy of the simulation for the objective of this study. Calculating the reaction force is very challenging because it depends on a very complex simulation of the behavior of the fluid while it is impacting the wall. This is illustrated in Figure 22, which shows the deformed shape of the light-frame wall and the corresponding stress demands at the moment of wave impact.

The four locations in Figure 22 with the highest stress demands, depicted by red and green fringes, correspond to wall supports that in the physical model were instrumented with load cells. Measured and calculated wall reactions during wave impact are presented in Figure 22, which shows that the FE model provided a very accurate representation of wave impact forces.

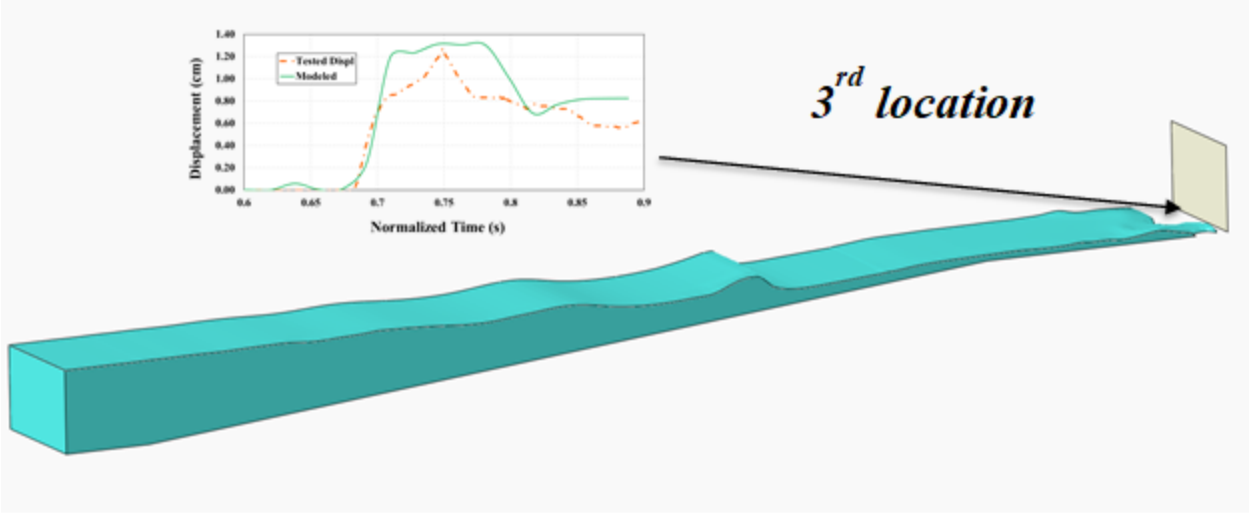

Figure 19. Location of control point 3 at the wall of tsunami wave impact model.

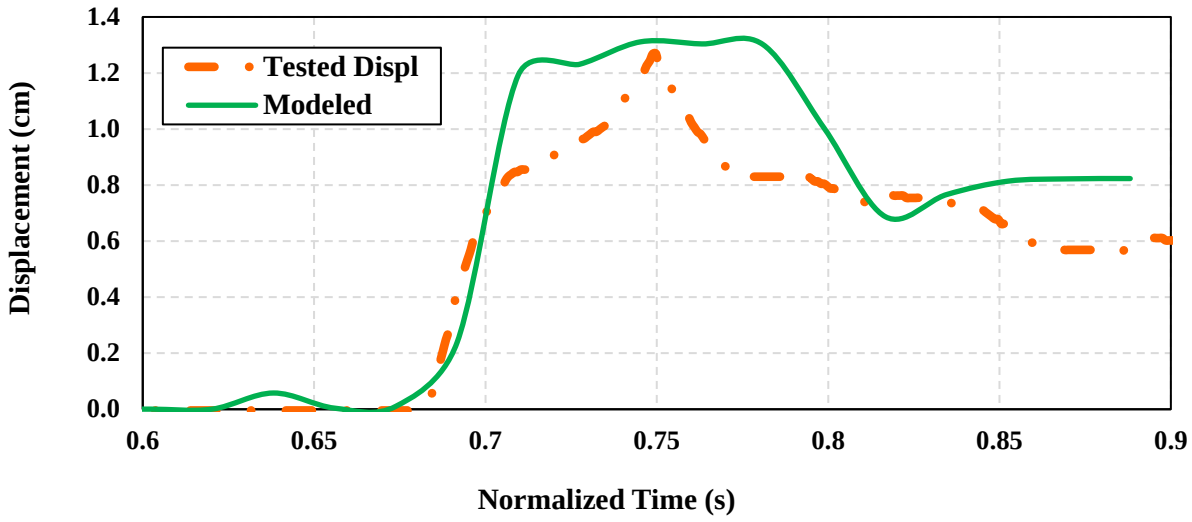

Figure 20. Measured and calculated wall displacement at control point 3 of tsunami wave impact model.

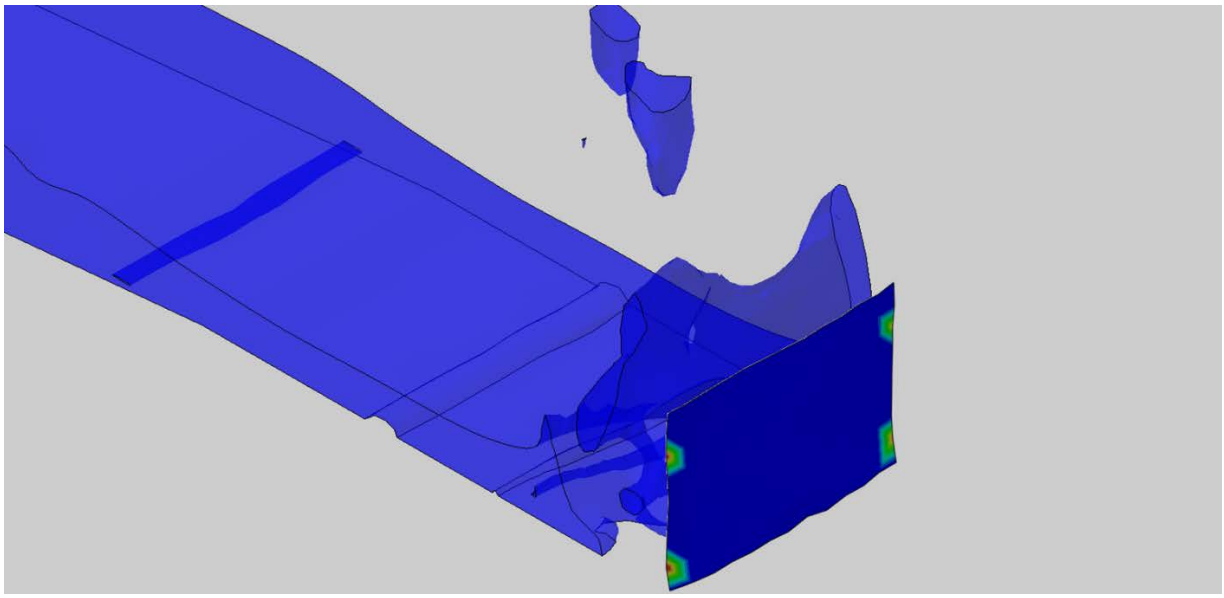

Figure 21. Stress distribution in light-frame timber wall during wave impact.

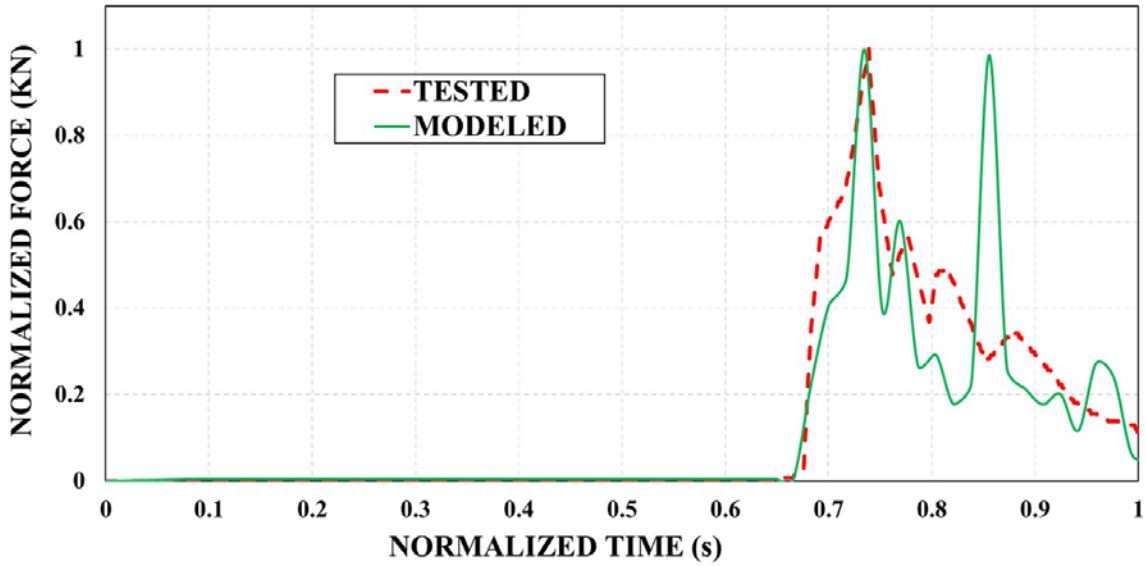

Figure 22. Measured and calculated wall reaction force for tsunami wave impact model.

5. FINDINGS

Having established confidence in the methodology to model wave impact forces on structures using CEL analysis in ABAQUS, a model of a causeway bridge structure that failed during hurricane Ivan *(1, 11)* was created to calculate support forces under representative hurricane loads. The model is representative of the I-10 bridge over Escambia Bay, Florida, and the dimensions are based on the original Florida DOT drawings. This bridge is of particular interest because there are at least two flume experiments replicating this particular configuration *(1)* and because one of these experiments was used to calibrate the empirical coefficients in the 2008 AASHTO guidelines for estimating wave-induced forces in bridges *(9)*. This model provides a basis for broader studies to create fragility relationships that provide the probability of reaching a specific bridge damage state for a given engineering design parameter. Those relationships are essential for studying and improving the resiliency of bridge infrastructure in the Gulf Coast region.

5.1. Bridge Causeway Model

The bridge causeway FE model was based on the Florida DOT plans of the I-10 bridge over Escambia Bay, Florida, which failed during hurricane Ivan. Using this bridge geometry was advantageous, because there are multiple flume experiments featuring this configuration, including a recent series of 1:5 scale experiments in the large wave flume at Oregon State University (OSU) *(1)*. In the OSU experiments, uplift forces were measured using load cells mounted in line with external offshore and onshore girders. It should be noted that only one test trial was used to verify uplift forces.

A layout of the modeled bridge is presented in Figures 24a and 24b. The bridge had a total of six AASHTO type III girders supporting the deck. The model tested in OSU's large wave flume was mounted through a reaction frame which provided rigid connections in the vertical direction and flexible connections in the horizontal direction. Horizontal flexibility was varied in the experiments through the use of springs with a range of flexibility constants. The springs simulated extremely flexible supports, the calculated flexibility of the substructure, and rigid supports. Reaction forces were measured using four vertically-oriented load cells and 2 horizontally-oriented load cells *(1)*.

In the FE model supports were modeled as rigid at the offshore corners and as simple supports at the onshore corners. Bridge girders and the deck were modeled using 3-D solid elements with overall dimension of 6.4 × 11.3 ft (1.94 × 3.45 m), using the same material properties presented in Table 7. The elastic modulus of the concrete was set to 4300 ksi (30 GPa). Material models, element types, and surface interactions were the same as those used in the tsunami calibration model. Similar to the tsunami calibration model, the Eulerian domain was divided in two volumes occupied by water and a void material. Results from the wave impact simulation are shown in Figures 25 to 30. Figure 25 shows a sequence of images illustrating the impact of the wave on the bridge structure at 12 discrete times. The wave initiated at time t_1 and reached maximum elevation over the bridge at time t_6. At time t_1, when the simulation started, the water level was representative of storm surge almost reaching the bottom surface of the prestressed girders. A closer view of the sequence of the wave impacting the bridge is presented in Figure 26, with the second image corresponding approximately to the wave location at time t_6.

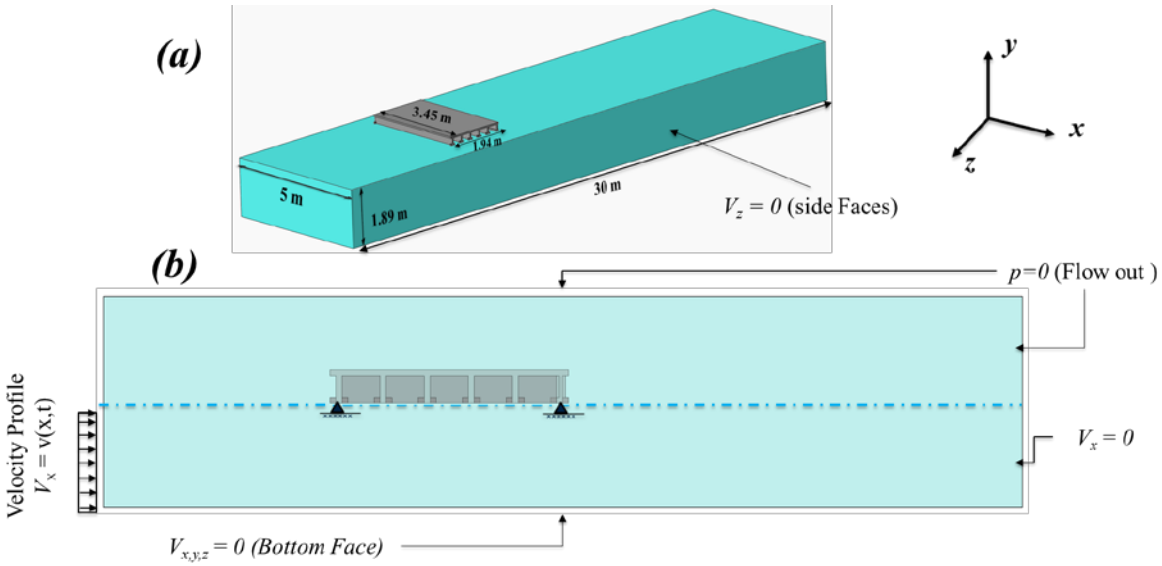

Figure 23. Causeway bridge model: (a) numerical model configuration (b) model boundary conditions.

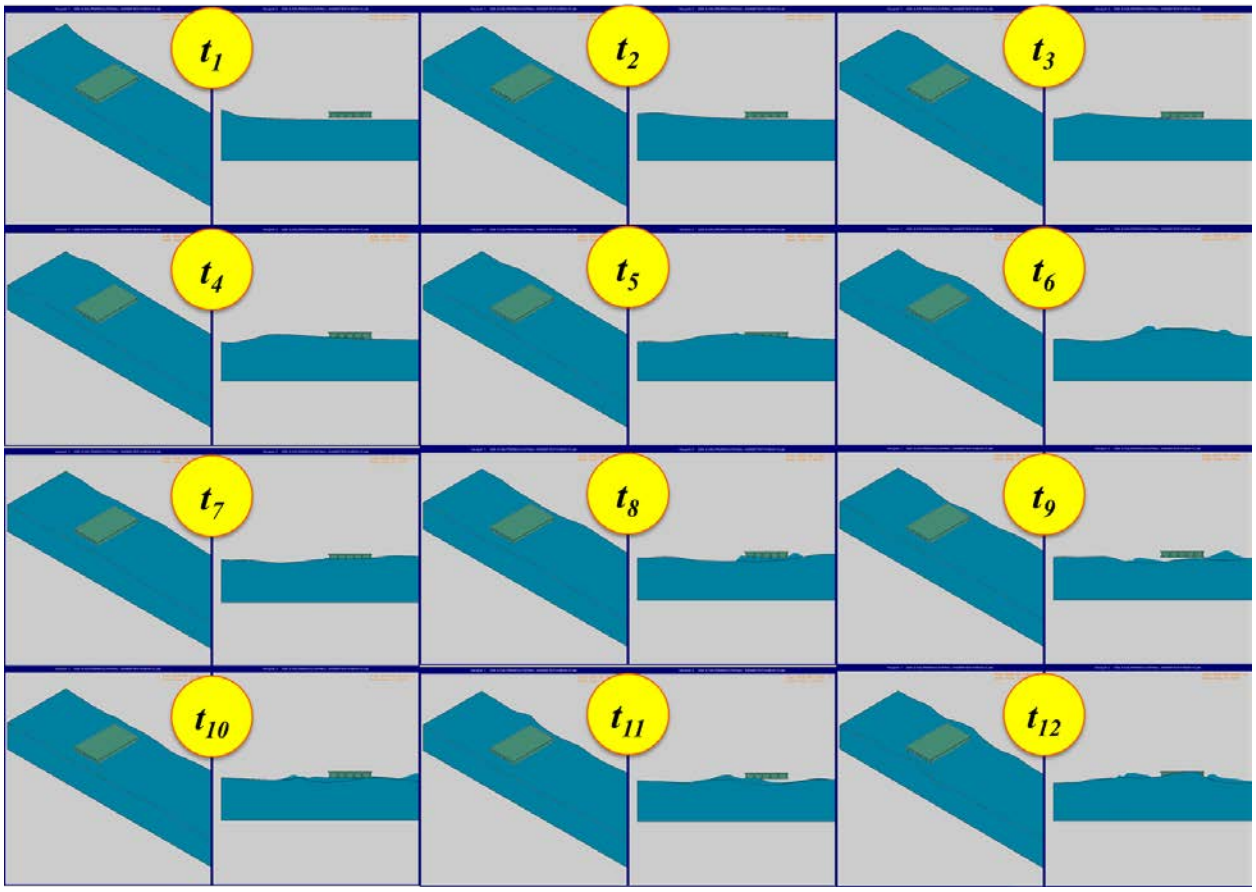

Figure 24. Wave impact sequence for bridge model.

Figure 27 shows that the maximum amplitude of the wave during the simulation, generated with an initial velocity of approximately 1 m/s, was approximately 0.3 m, which adjusted using

similitude laws correspond to a prototype wave amplitude of 1.5 m. The period of the wave in the model was approximately 1 sec. which scaled using Froude criteria corresponds to a prototype wave period of 2.3 seconds. Researchers have estimated that wave heights in Escambia Bay during hurricane Ivan were as high as 2.6 m, and that wave periods were as high as 7 seconds, so the wave modeled was well within the range expected in a catastrophic event in the Gulf region *(1)*.

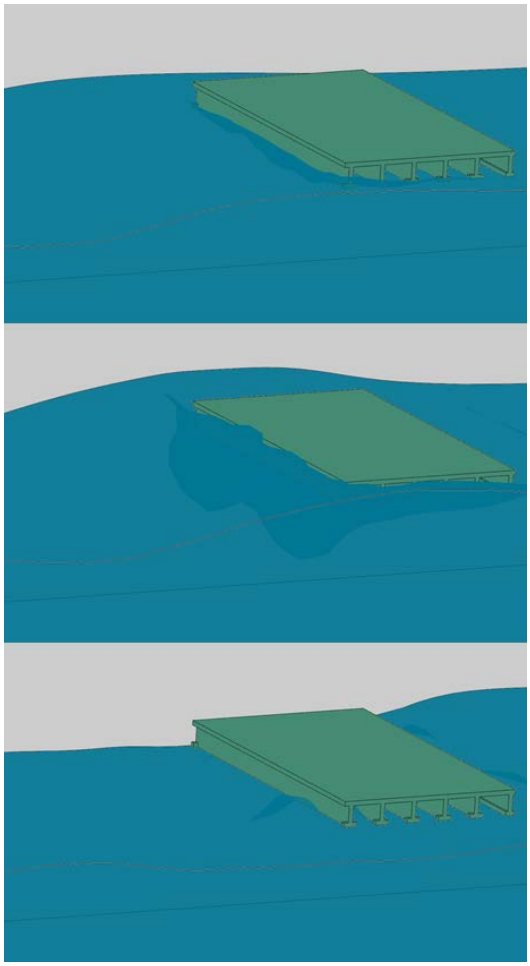

Figure 25. Wave impact sequence for causeway bridge model.

Computer simulation results were compared with results from one of the flume experiments performed at OSU to verify that material models used in the calibration model were adequate for the simulation of the bridge response. A comparison between measured and calculated reaction force in the bridge is presented in Figure 28 during the time segment with highest force demand, which shows that there was a close correlation between measured and calculated values.

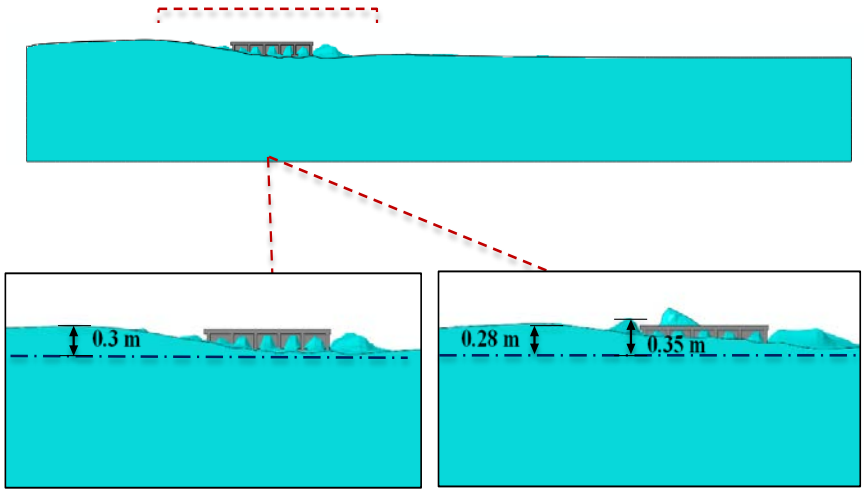

Figure 26. Profile of wave impact simulation on causeway bridge showing wave elevations prior to impact.

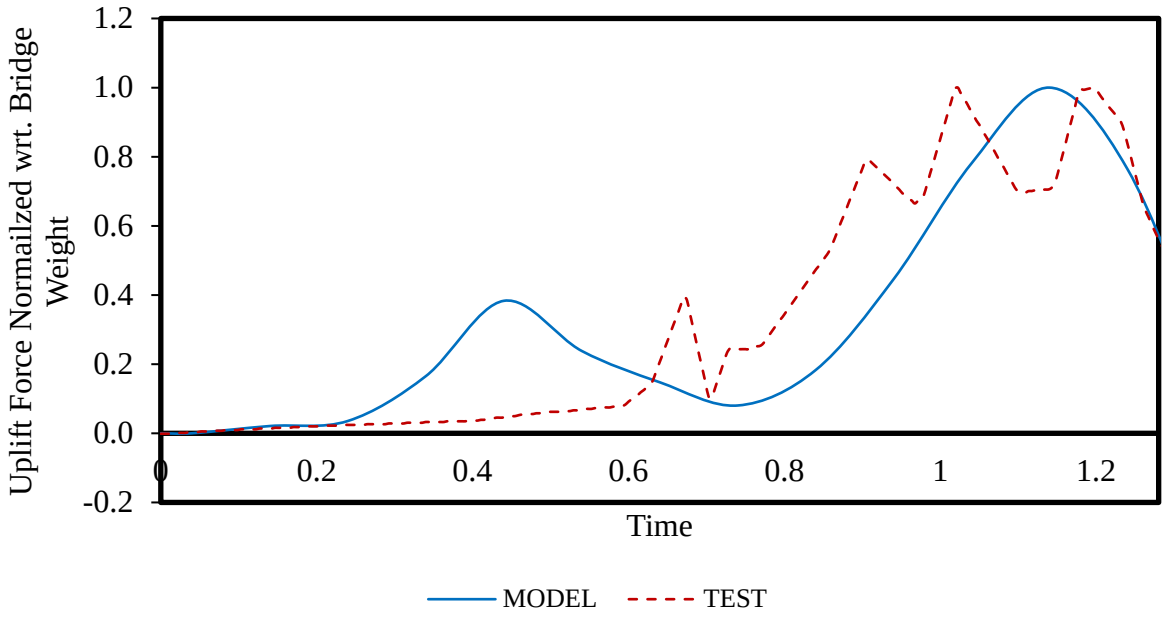

Figure 27. Normalized vertical force vs time for bridge model.

Having established that the model provided an accurate representation of the bridge support forces, several other simulation results are presented in Figures 30 and 31. Figure 30 shows water velocity at control locations 1, 2, and 3, shown in Figure 29, at points before (locations 1 and 2) and after the bridge. Velocity values in Figure 30 show that the turbulent flow near in the vicinity of the bridge leads to much higher velocities at locations 2 and 3 than those calculated at location 1, away from the bridge.

The magnitude of the reaction force normalized with respect to bridge weight is presented in Figure 31. Three different graphs are presented in Figure 31, the first corresponding to reaction force

resultant, the second corresponding to the horizontal hydrodynamic force, and the third corresponding to the uplift force. For the wave conditions simulated, with wave amplitudes much lower than those that occurred during hurricane Ivan, the magnitude of the reaction force and the uplift force exceeded the weight of the bridge. Figure 31 also shows that for these particular wave characteristics and bridge support conditions the horizontal reaction due to hydrodynamic forces was as high as 60% of the weight of the bridge, which would impose a very large demand on shear keys if employed as a measure to improve the resilience of the bridge. It is important to keep in mind that bridge supports in the FE model were modeled as rigid, and that measurements with flexible supports that simulate the flexibility of the substructure have been shown to be significantly lower *(1)*. The magnitude of the calculated support demands suggest that significant damage would be expected to occur for the hydrodynamic conditions in the simulation, which is consistent with the fact that the bridge structure collapsed during hurricane Ivan, although more simulations that include the flexibility of the substructure should be performed to obtain more accurate estimates of actual bridge conditions.

Although the scope of this project does not include the development of fragility relationships, the model developed and calibrated in this study can be used to develop such relationships, and to provide guidance on the level of damage expected for a wider range of hydrodynamic demands.

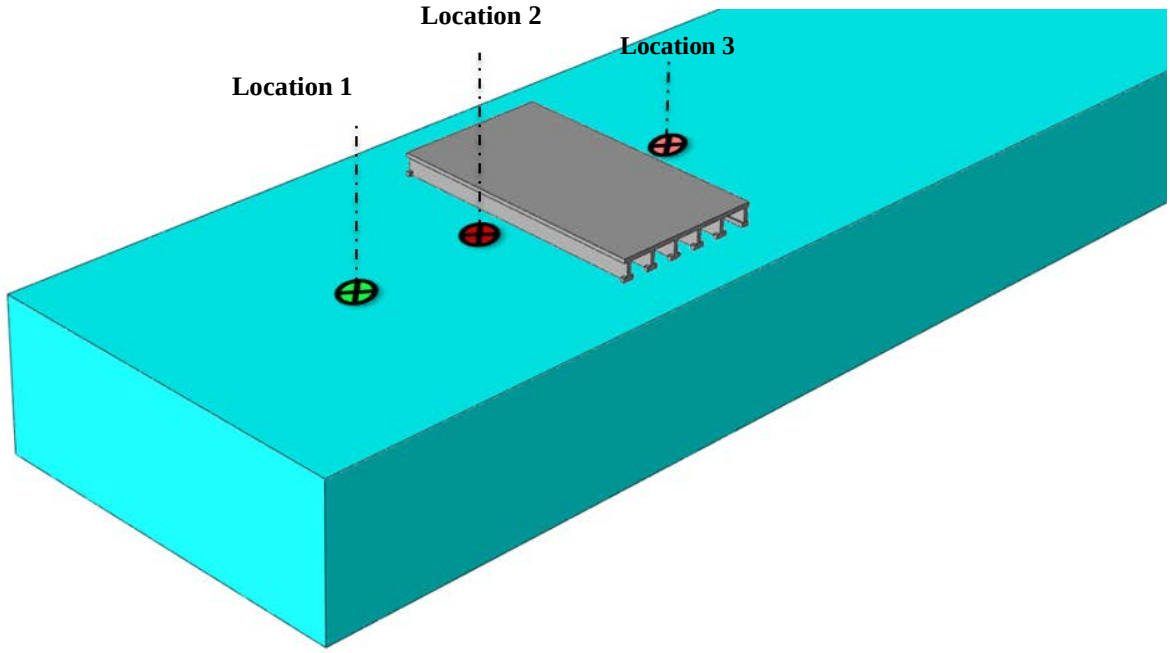

Figure 29. Locations 1, 2, and 3 for monitoring of wave velocity.

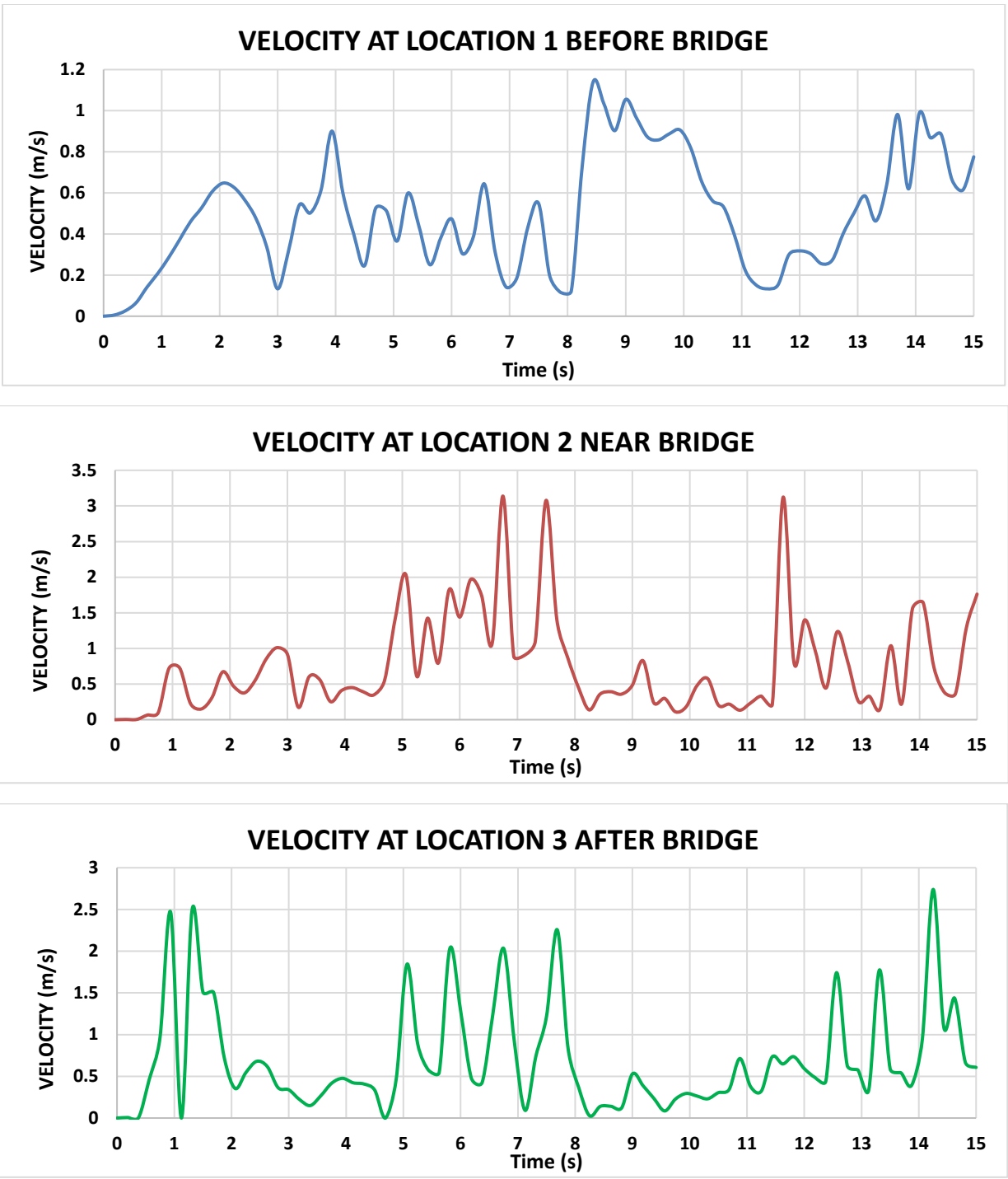

Figure 28. Calculated water velocity at locations 1, 2, and 3 in Figure 29.

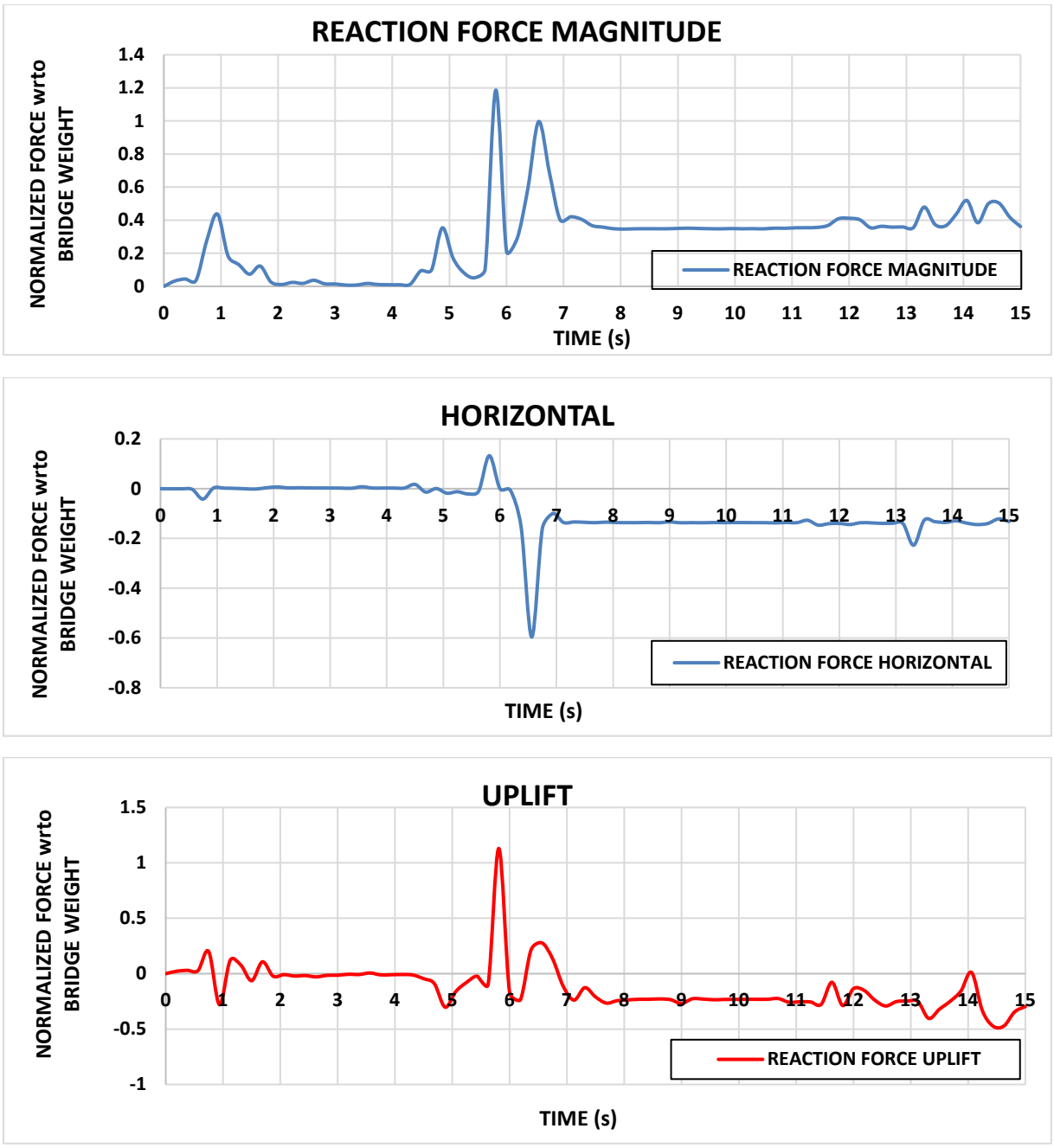

Figure 29. Calculated support reactions normalized with respect to bridge weight.

5.2. Parametric Analysis

Informed by the results for the literature review and having completed the calibration of the causeway bridge model, a parametric study was performed to evaluate the effect of two different types of hydrodynamic loads and substructure conditions on connection demands. Damage from hurricanes in the Gulf coast to bridge structures during Hurricanes Ivan (I-10 bridge over Escambia Bay) *(1)* and Katrina (twin span bridge over Lake Pontchartrain) *(5)* is well-documented in the literature review. Furthermore, this problem has also occurred under different hydrodynamic loading conditions, during recent flash floods in Austin, TX (Kingsland bridge over Llano River

on 16 October 2018) and San Marcos, TX (Fischer Store Rd. over Blanco River on 23 May 2015). The main mode of failure of bridge structures in these flash floods and hurricanes was unseating of the superstructure, which was occurred in bridges with different types of support connectivity *(5)*. It is a common assumption in bridge design that short duration slamming forces are not a concern for the design of the substructure, but it is not clear if these forces can cause significant damage to superstructure connections, eventually leading to the collapse of the bridge superstructure. These types of loads are of significant concern, for example, in blast-resistant design, where short-duration loads have been shown to damage façade element connections. An important factor for consideration in regards to short-duration forces is that flume tests performed by Bradner *(1)* and others at Oregon State and computer simulations by Istrati and Buckle *(28)* showed that substructure flexibility has a very significant effect on the magnitude of hydrodynamic "slamming" wave forces, and this effect is not considered in current design equations.

Simulations in the parametric study included models with and without substructure piers (Figure 32), and two different types of hydrodynamic forces, representative of wave impact simulated in research studies by Brandner, Do and Gullett *(1, 11, 18)*, and sudden surge as used in the study by Bricker *(31)*. In models in which the substructure was not simulated (Figure 32), the bridge superstructure was constrained by rigid supports, an assumption that is common in both computational models used by researchers and physical models tested in flumes *(1, 11, 18)*. In models in which the substructure was included in the simulation (Figure 32), the superstructure was tied to a cap beam that was attached to four bridge piers fixed at the base. Although this is a more realistic model, it does not account for flexibility of the pile foundation, which would significantly increase the computational cost. Accounting for the flexibility of the foundation is important, and should be the subject of future studies.

Connections were not modeled explicitly to reduce computational cost, but it is expected that vertical forces exceeding the weight of the bridge and horizontal forces exceeding the friction force expected in bridge supports would lead to unseating of the superstructure in simply-supported bridges. For reference, the coefficient of friction between clean concrete surfaces is approximately 0.6 and the coefficient of friction between steel surfaces is approximately 0.7, both of which decrease significantly under dynamic conditions. As shown in Figure 2, many costal bridges have simple pinned supports to accommodate thermal expansions and are particularly susceptible to unseating. Vertical forces exceeding the weight of the bridge would necessitate anchorage of the bridge. Establishing the need for shear keys is more complicated because the amount of horizontal force needed to initiate motion is highly dependent on the type of superstructure connection and may be reduced by uplift forces, but if the contribution of the connection to lateral force resistance is neglected shear keys should be proportioned to resist the totality of the lateral force.

5.3. Wave Impact Analyses

The objective of the parametric study was to be able to compare connection forces for two different types of hydrodynamic forces and two different bridge configurations, including and excluding the effect of substructure flexibility. Figure 33 illustrates results from a suite of simulations of wave impact with three different wave initial velocities, for the bridge configuration without piers. A similar set of simulations was performed for the bridge configuration with piers.

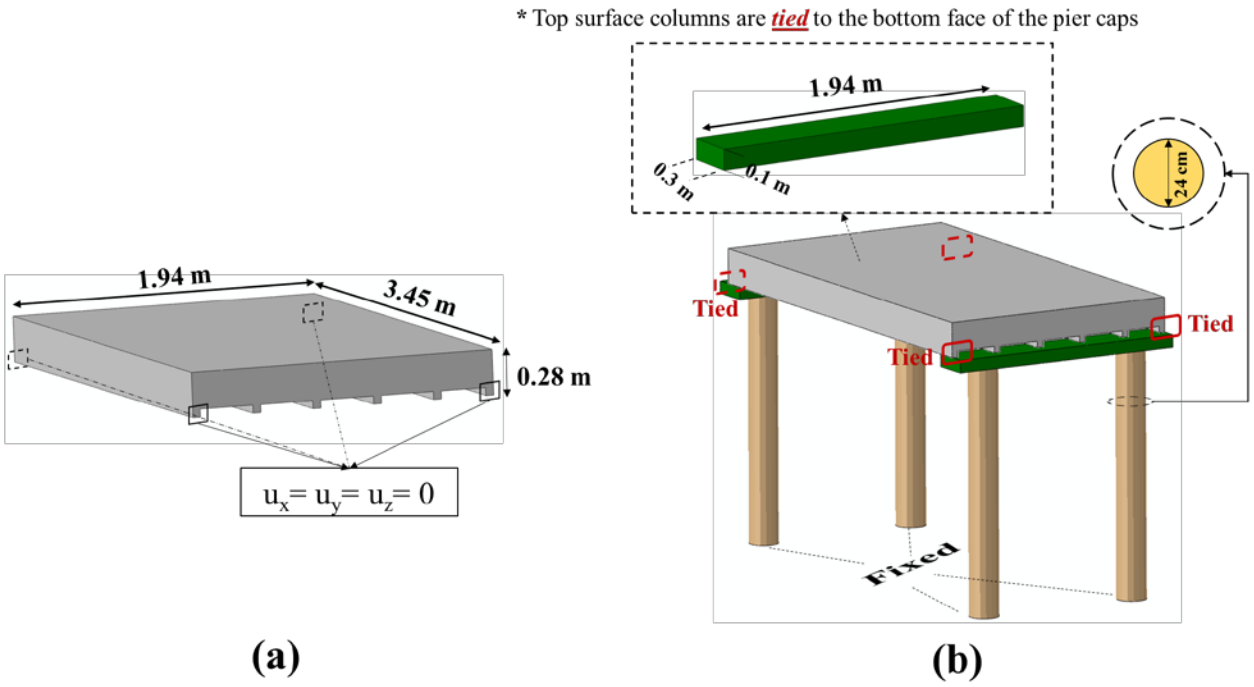

Figure 30. Bridge models used in parametric study.

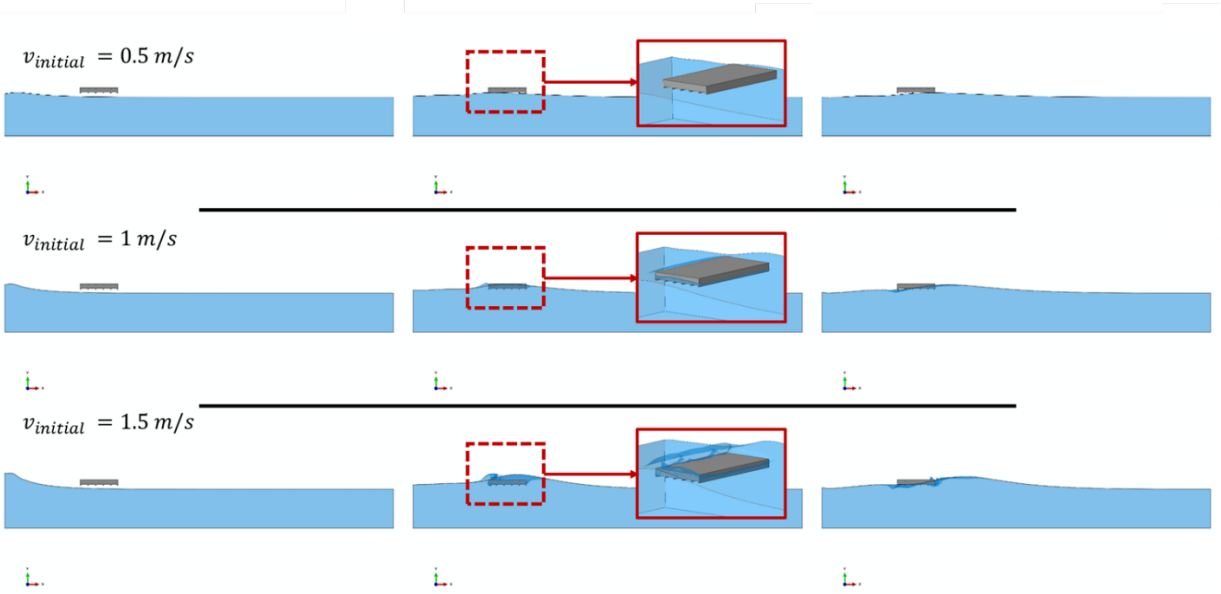

Figure 31.Wave impact for model without piers.

Calculated connection forces normalized with respect to the bridge weight are presented in Figure 34 for the three wave initial velocities, and the two different bridge configurations. Vertical forces shown in Figure 34 include the weight of the bridge, so magnitudes below zero indicate that the uplift force was not large enough to displace the superstructure by itself. It is important to note that the analysis results do not include the effects of buoyancy, which would increase the magnitude of the uplift force. Also, uplift forces reduce the magnitude of gravity loads, which reduces the normal

force across the support. In bridge structures supported on steel plates or pin supports a reduction in the normal force across the connection creates a reduction in the friction force that prevents horizontal displacement through the connection.

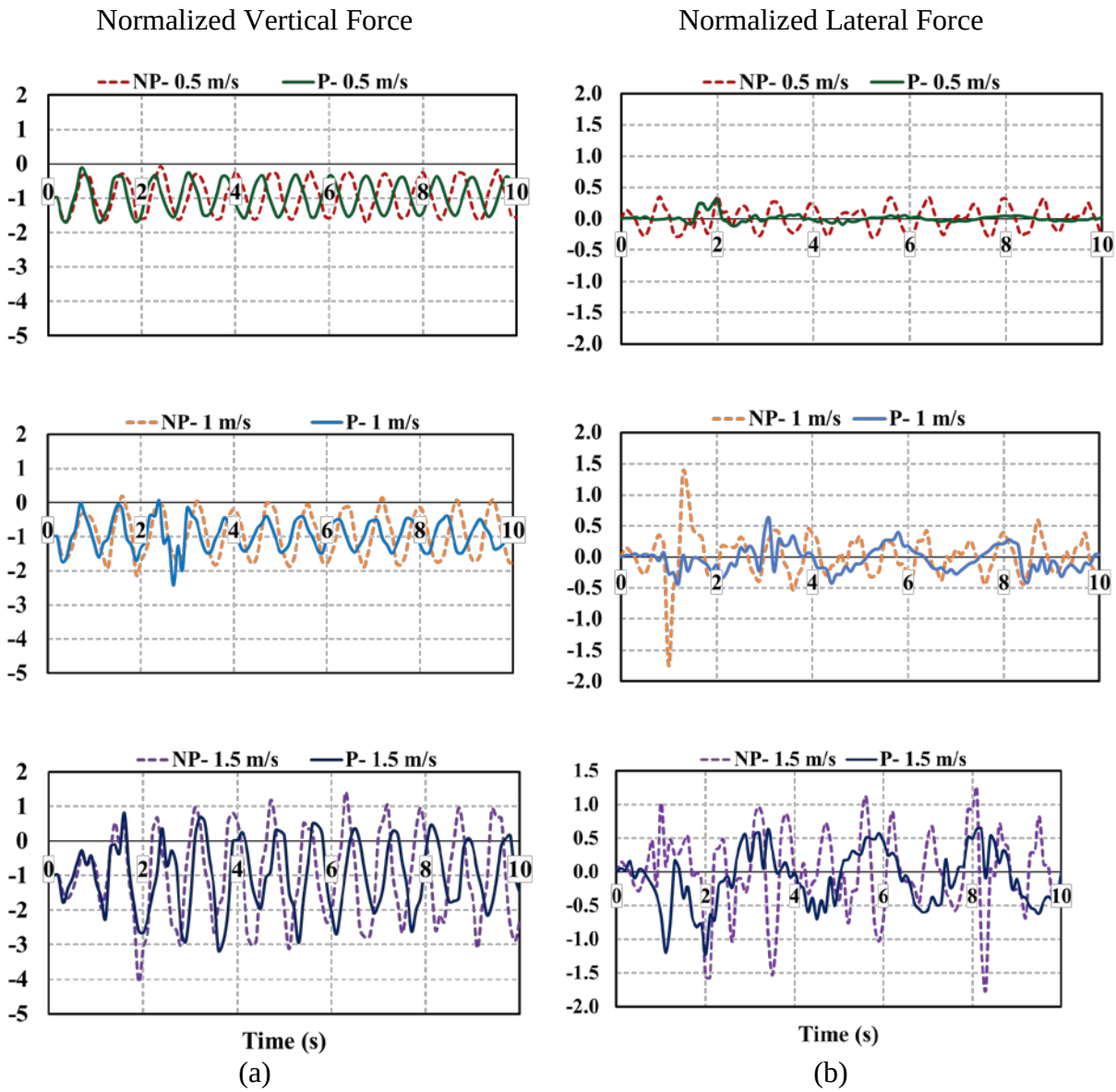

Figure 32. Horizontal and vertical forces for bridge models subjected to wave impact.

The results in Figure 34 show that the difference between the normalized vertical force of the models with and without piers increased with wave velocity and amplitude. Of the three models evaluated, only the model with an initial velocity of 1.5 m/s had vertical forces exceeding the weight of the bridge, although the other two models reached a net force of nearly zero. The wave with an initial velocity of 1 m/s correspond to the calibration case, and a prototype wave amplitude of approximately 1.5 m. The difference in the horizontal force calculated for the models with and without piers increased with wave velocity and amplitude. Peak values for the model with an initial velocity of 0.5 m/s were approximately the same for both models, and remained below 30% of the bridge weight. Horizontal forces for the two higher initial velocities were significantly lower for

the model that included substructure flexibility (Figure 34). For the models with an initial velocity of 1.0 m/s the ratio of peak horizontal forces between models with and without foundation flexibility was approximately 2.8, while in the models with an initial velocity of 1.5 m/s the ratio was approximately 1.4. While the peak lateral force in the model with foundation increased in proportion to initial velocity at the boundary, in the model without foundation flexibility the peak force was nearly the same for initial boundary velocities of 1.0 and 1.5 m/s.

5.4. Analyses for Rapidly Rising Storm Surge

A second set of simulations was conducted for different hydrodynamic loading conditions. In this evaluation an initial velocity of 1 m/s was applied to the entire fluid domain. The boundary conditions at the outlet and inlet were adjusted to cause the water level to rise rapidly (Figure 35). While the velocity at the outlet surface was set constant to 1 m/s throughout the analysis, the velocity at the inlet surface increased linearly from 1 to 2 m/s over a time period of 32 seconds. A lateral velocity of zero was specified at the sides of the fluid domain to prevent water running off the domain. For the bridge model without piers the rear end and the front supports were restrained from horizontal displacement (pinned support). In the bridge model that included piers, superstructure locations restrained from lateral movement in the model without piers were attached to the pier caps using tie constraints. The pier caps were attached to the top of pier surfaces also through tie connections, and the bottom surface of the piers was fully fixed (Figure 32).

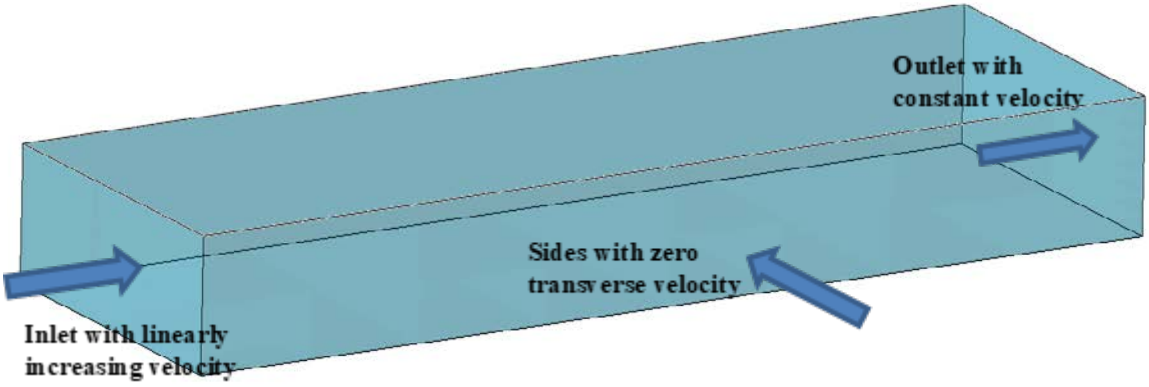

Figure 33. Boundary conditions for model with rapidly increasing water level.

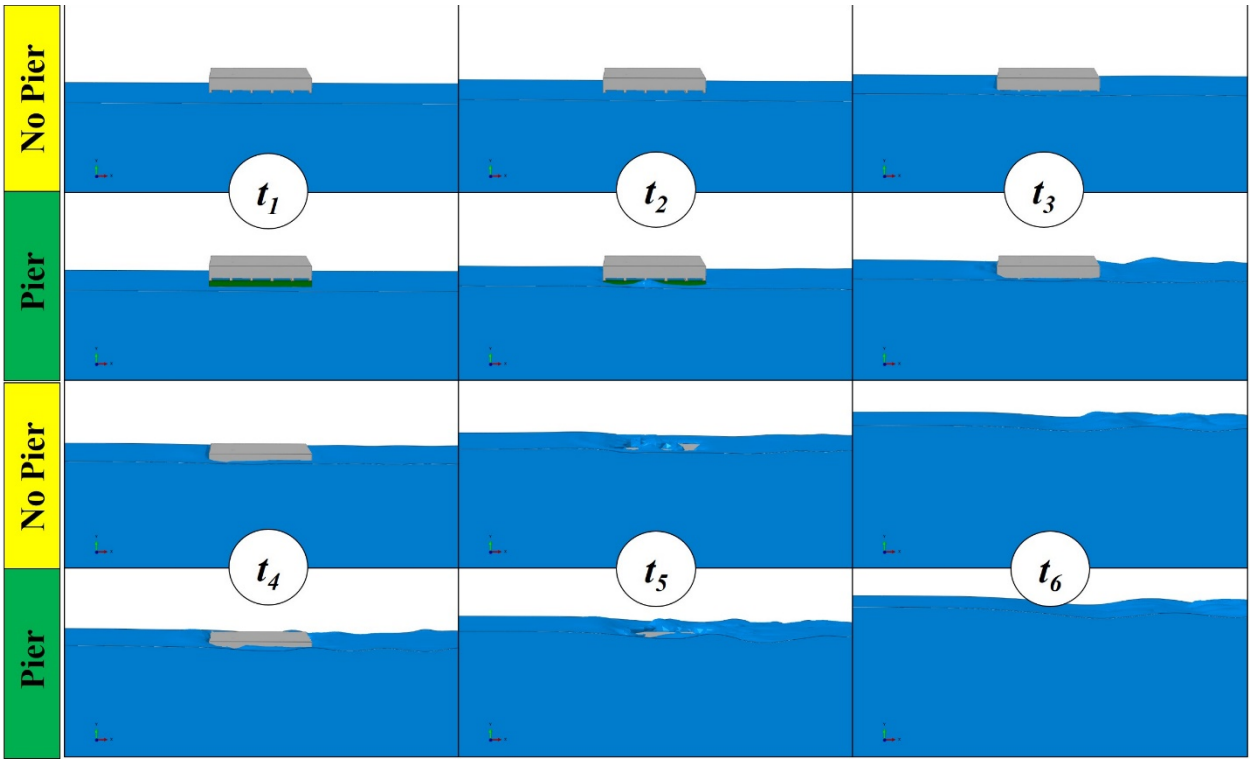

Figure 34. Simulation with raising water level and constant water velocity field.

Results from the two simulations corresponding to models with and without piers are illustrated in Figures 36 through 38. Figure 36 shows the response of the bridge structure at 6 discrete points in time, from the initiation of the simulation (t_1) to a time when the bridge is completely submerged (t_6).

For these different sets of hydrodynamic loading conditions, the effect of foundation flexibility was significantly different. Vertical forces acting on the connection increased with rising velocity and water level, but their peaks had similar magnitude, regardless of foundation flexibility. These results suggest that the vertical response of the bridge was dominated by the vertical flexibility of the piers, which is very high, so the assumption of a vertical constraint did not affect the accuracy of the results. In the case of the horizontal force, the difference between the model with piers and the model without piers increased with increasing velocity. These results suggest that the lateral flexibility of the bridge had a significant effect on the dynamic response of the bridge, and that the assumptions of rigid supports is an inadequate approximation.

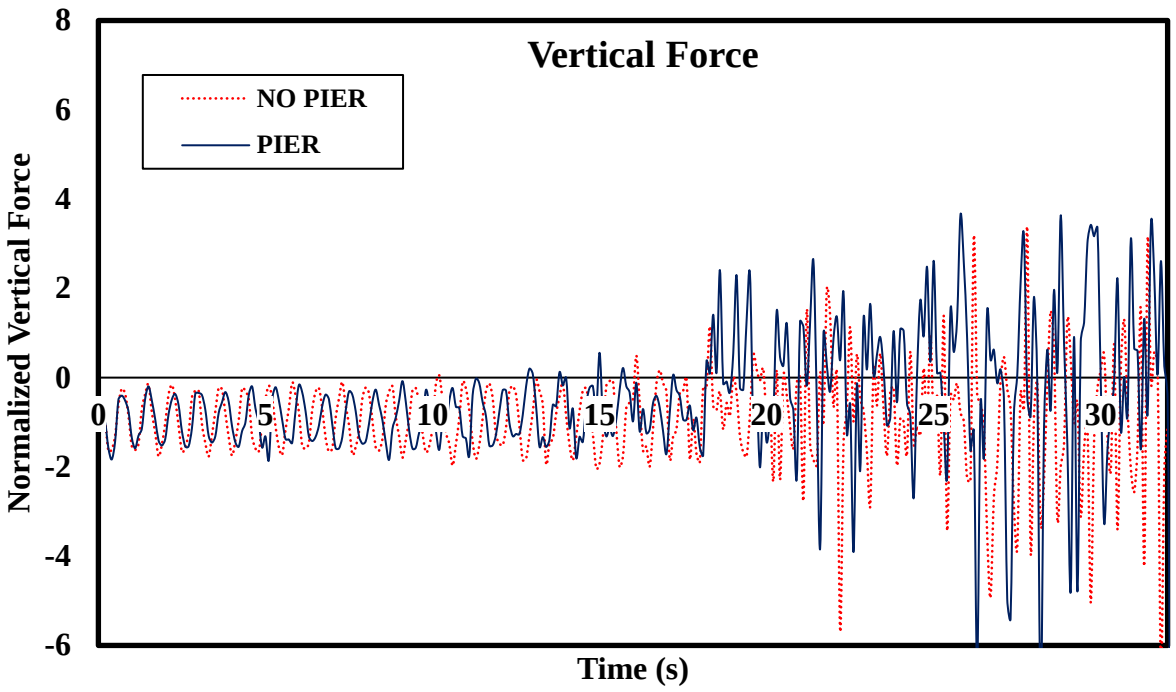

Figure 35. Normalized vertical connection force for simulation with rapidly raising water level.

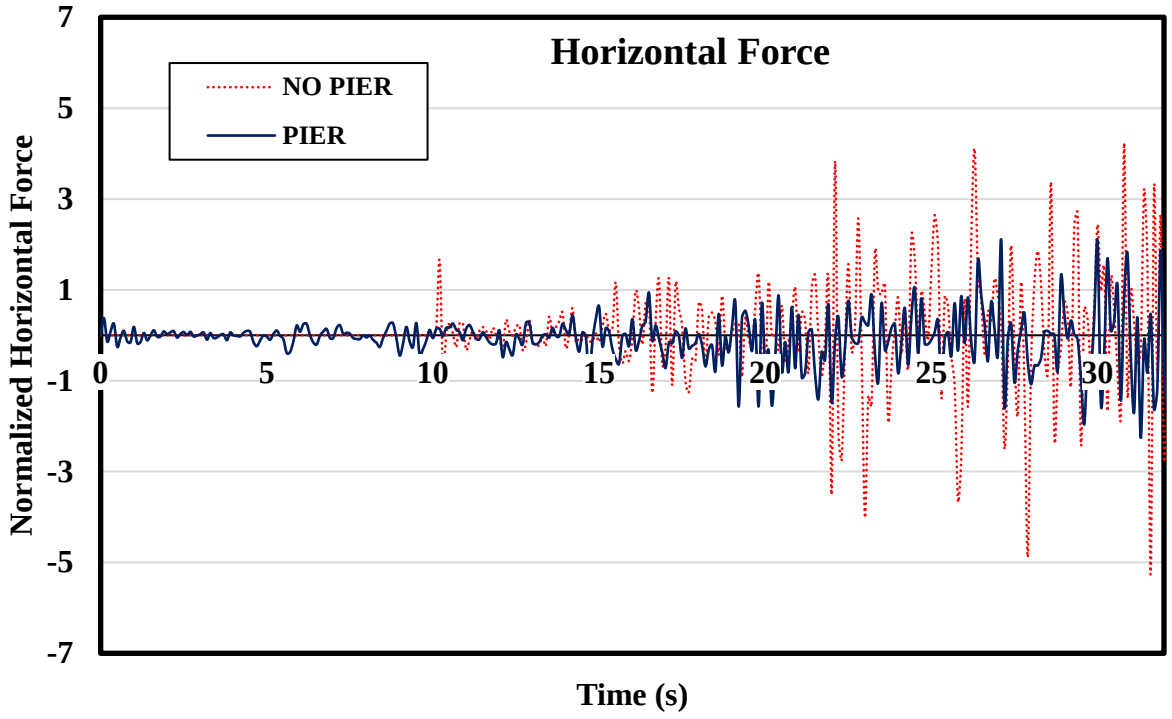

Figure 36. Normalized horizontal connection force for simulation with rapidly raising water level.

6. CONCLUSIONS

High-resolution finite element models were developed to study the effect of wave-impact forces on transportation infrastructure in the Gulf Coast region during large storms. Simulation results showed that Coupled Eulerian-Lagrangian analysis was effective for calculating accurate estimates of hydrodynamic forces during wave impact, and can be used to evaluate the expected level of damage on bridge structures during hurricanes.

The modeling technique and parameters were successfully calibrated and evaluated using results from two different flume experiments. The first flume experiment evaluated the magnitude of wave impact forces on a light-frame structure induced by a Tsunami wave. Simulation results provided accurate estimates of wave height, water velocity, wave impact force, and wall deformation recorded during the experiment.

An FE model of an I-10 bridge in Escambia Bay that failed during hurricane Ivan was also created. Results from the computer model were evaluated using measurements from a 1:5 scale flume test of the bridge and found to provide accurate estimates of the measured force on the bridge supports during wave impact.

An FE simulation of the I-10 Escambia Bay bridge under a wave configuration representative of a large hurricane showed that this type of storm can induce forces sufficiently large to cause the collapse of the bridge superstructure due to unseating, as it actually occurred during hurricane Ivan. Uplift forces calculated with the assumption of rigid supports exceeded the weight of the bridge and the horizontal force was as high as 60% of the weight of the bridge. Those results indicate a large probability of severe distress for bridges with simple connections under the type of hydrodynamic loads simulated due to uplift or unseating of the supports. These results also indicate that even if shear keys are used to mitigate the potential damage, either in an original design or as a retrofit measure, the shear keys must be proportioned to resist the large horizontal force demands expected in the bridge. It is important to emphasize that the models evaluated were intended to match laboratory tests with rigid supports, and that experimental data has shown that substructure flexibility can lead to significant reductions in superstructure support demands.

The parametric study that was conducted showed that foundation flexibility affects the magnitude of calculated hydrodynamic forces, and most significantly the effect of short duration slamming forces. The parametric study also showed that the effect of foundation flexibility is sensitive to the type of hydrodynamic loads imposed on the bridge, and that it affects differently the horizontal and vertical forces acting on the superstructure connection.

7. RECOMMENDATIONS

The main objective of the project was to develop a high-resolution FE model to study the magnitude of wave impact forces on bridge structures during large hurricanes in the Texas-Louisiana Gulf Coast region. The scope of project consisted of developing two FE models to validate the analysis methodology using experimental results, and to perform a simulation that would provide estimates of bridge support demands representative of wave configurations expected during a major hurricane in the Gulf Coast region.

The simulations performed in this study represent a fundamental step towards a better understanding of the risk to bridge infrastructure in the Gulf Coast due to hurricanes, and towards improving the resiliency of bridge infrastructure. The methodology evaluated and the type of models created can be used to study effect of engineering parameters related to wave configuration on expected support demands and bridge damage. Bridge configuration parameters to be evaluated include water elevation, wave height, wave period, wave directionality and wave length. It is also important to study the effect of bridge configuration on support demand, including bridge geometry, support type, substructure configuration, and bridge span.

The results from this study showed that computer and physical models of bridge structures that do not include the effect of substructure flexibility on fluid-structure interaction may significantly overestimate short-term duration forces, so it is important to include this effect on improved formulations to estimate hydrodynamic forces.

REFERENCES

1. Bradner, C., Schumacher, T., Cox, D. and Higgins, C., "Experimental Setup for a Large-Scale Bridge Superstructure Model Subjected to Waves," Journal of Waterway, Port, Coastal, and Ocean Engineering, ASCE, Vol. 137, No. 1, January 1, 2011.

2. State of Texas, Office of the State Demographer, T. S. D. C. The University of Texas at San Antonio, Austin, TX, 2014.

3. Trucknews. "Transportation Infrastructure is Decimated by Katrina," http://www.trucknews.com/features/transportation-infrastructure-is-decimated-by-katrina/, last accessed 6/10/2018.

4. U.S. Department of Transportation. "Beyond Traffic 2045," https://www.transportation.gov/sites/dot.gov/files/docs/BeyondTraffic_tagged_508_final.pdf, last accessed 12/13/2018.

5. Padgett, J., Des Roches, R., Nielson, B., Yashinsky, M., Kwon, O., Burdette, N., and Tavera, E, 2009. "Bridge Damage and Repair Costs from Hurricane Katrina," Journal of Bridge Engineering, ASCE, Vol. 13, No. 1, 2009.

6. America 2050. "Megaregions," http://www.america2050.org/content/megaregions.html, last accessed 12/13/2018.

7. American Association of State Highway and Transportation Officials. "AASHTO LRFD Bridge Design Specifications," 8th Edition, Washington DC. , 2017

8. Department of the Army. "Shore Protection Manual," Coastal Engineering Research Center, Waterways Experiment Station, Corps of Engineers, Vicksburg Mississippi, 1984.

9. AASHTO. "Guide specifications for bridges vulnerable to coastal storms (BVCS-1)", Washington, D.C., 2008.

10. Almasri, A., and Moqbel, S., "Drag Force Coefficients of Water Flow Around Bridge Piers," Journal of Engineering Materials and Technology, 139(2) (2017) 021001.

11. Do, T.Q., van de Lindt, J.W., and Cox, D.T. "Performance-based design methodology for inundated elevated coastal structures subjected to wave load," Engineering Structures, 117, 2016, pp. 250-262.

12. Como, A. and Mahmoud, H., "Numerical evaluation of tsunami debris impact loading on wooden structural walls," Engineering Structures 56. 2013 1249-1261.

13. Sato, M. and Kobayashi, T. "A fundamental study of the flow past a circular cylinder using Abaqus/CFD," 2012 SIMULIA Community Conference, 2012.

14. Smojver, I. and Ivančević, D. "Bird strike damage analysis in aircraft structures using ABAQUS/Explicit and coupled Eulerian Lagrangian approach," Composites Science and Technology 71(4), 2011, pp. 489-498.

15. Bai, D., Chen,G., and Wang, Z. “Seismic response analysis of the large bridge pier supported by group pile foundation considering the effect of wave and current action,” The 14th world conference on earthquake engineering, Beijing, China, 2008.

16. Chiarelli, M., Ciabattari, R., Cagnoni, M., and Lombardi, G., “Fluid-Structure Interaction Analyses of Wings with Curved Planform: Preliminary Aeroelastic Results,” CEAS 2013, LINKÖPING, Sweden 2013.

17. Chiarelli, M., Ciabattari, R., Cagnoni, M., and Lombardi, G., “The effects of the planform shape on drag polar curves of wings: fluid-structure interaction analyses results,” STAR Global Conference 2013, CD-Adapco, 2013, pp. 101-123.

18. Gullett, P., Dickey, M., and Howard, I. “Numerical Modeling of Bridges Subjected to Storm Surge for Mitigation of Hurricane Damage,” Southeast Region Research Initiative (SERRI) Rep. 70015-005, Rep., US Department of Homeland Security Directorate, 2012.

19. Bozorgnia, M. and Lee, J.,” Computational Fluid Dynamic Analysis of Highway Bridges Exposed to Hurricane Waves,” Coastal Engineering Proceedings 1(33). 2012. 70.

20. Sewell, D. “Wave loads on multi-member offshore wind turbine sub-structures,” University of Delaware, 2012.

21. Bozorgnia, M. and Lee, J. and Raichlen, F. “Wave Structure Interaction: Role of Entrapped Air on Wave Impacts and Uplift Forces,” Coastal Engineering Proceedings 1(32). 2011. 57.

22. Erduran, K., Seckin, G., Kocaman, S. and Atabay, S. “3D Numerical Modelling of Flow Around Skewed Bridge Crossing,” Engineering Applications of Computational Fluid Mechanics 6(3), 2012, pp. 475-489.

23. Lau, T.L., Ohmachi, T., Inoue, S. and Lukkunaprasit, P. “Experimental and Numerical Modeling of Tsunami Force on Bridge Decks,” in Tsunami-a growing disaster, InTech2011, 2011.

19. Kocaman, S., Seckin, G., Erduran, K. “3D model for prediction of flow profiles around bridges,” Journal of hydraulic research 48(4), 2010, pp. 521-525.

24. Zong, Z., Xia, Z., Liu, H., Li, Y. and Huang, X. “Collapse Failure of Prestressed Concrete Continuous Rigid-Frame Bridge under Strong Earthquake Excitation: Testing and Simulation,” Journal of Bridge Engineering 21(9), 2016, 04016047.

26. Istrati, D., Buckle, I., Lomonaco, P., Yim, S. and Itani, A. “Tsunami Induced Forces in Bridges: Large-scale Experiments and The Role of Air-entrapment,” Coastal Engineering Proceedings 1(35), 2017, 30.

27. Azadbakht, M. and Yim, S.C., “Estimation of Cascadia Local Tsunami Loads on Pacific Northwest Bridge Superstructures,” Journal of Bridge Engineering 21(2). 2015 04015048.

28. Istrati, D., and Buckle, I. "Effect of fluid-structure interaction on connection forces in bridges due to tsunami loads." Proc 30th US-Japan Bridge Engineering Workshop, Washington DC, United States, 2014.

29. Shahbaboli, A. “Numerical Modeling of Extreme Flow Impacts on Structures,” Université d'Ottawa/University of Ottawa, 2016.

30. Chen, L., Zang, J., Hillis, A., Morgan, G., and Plummer, A. “Numerical investigation of wave– structure interaction using OpenFOAM,” Ocean Engineering 88. 2014. 91-109.

31. Bricker, J., Kawashima, K., and Nakayama, A. “CFD analysis of bridge deck failure due to tsunami”, Proceedings of the international symposium on engineering lessons learned from the Great East Japan Earthquake, March 1-4, 2012, Tokyo, Japan, 2012, pp. 1-4.

32. Xu, G. and Cai, C., “Numerical investigation of the lateral restraining stiffness effect on the bridge deck-wave interaction under Stokes waves,” Engineering Structures 130, 2017, pp. 112-123.

33. Zhang, X., Chen, X., Huang, J., Zhou, H., and Wang, Q. “Optimum Design of Bridge Cross Section with Low Clearance Considering Wave Load Effects Based on Numerical Wave-Tank,” Journal of Coastal Research 73(sp1), 2015, pp. 232-237.

34. Xu, Guoji, and C. S. Cai. "Numerical simulations of lateral restraining stiffness effect on bridge deck–wave interaction under solitary waves." Engineering Structures 101, 2015, pp. 337-351.

35. Qian-hui, L. and Zheng-xin, Z. “Traveling Wave Effect Analysis on Fabricated Box Girder Bridge Based on ANSYS,” Applied Mechanics and Materials, 2014.

36. Debus, K., Berkoe, J., Rosendall, B. and Shakib, F. “Computational fluid dynamics model for Tacoma narrows bridge upgrade project,” ASME/JSME 2003 4th Joint Fluids Summer Engineering Conference, American Society of Mechanical Engineers, 2003, pp. 179-184.

37. Shadloo, M., Oger, G., and Le Touzé, D. “Smoothed particle hydrodynamics method for fluid flows, towards industrial applications: Motivations, current state, and challenges,” Computers and Fluids 136, 2016, pp. 11-34.

38. Wei, Z., Dalrymple, R. Hérault, A., Bilotta, G., Rustico, E., and Yeh, H. “SPH modeling of dynamic impact of tsunami bore on bridge piers,” Coastal Engineering 104, 2015, pp. 26-42.

39. Zhang, A., Yang, W., Huang, C., and Ming, F. “Numerical simulation of column charge underwater explosion based on SPH and BEM combination,” Computers and Fluids 71, 2013, pp. 169-178.

40. Liu, M., Liu, G., Lam, K., and Zong, Z. “Smoothed particle hydrodynamics for numerical simulation of underwater explosion,” Computational Mechanics 30(2), 2003, pp. 106-118.

41. Liu, M., Liu, G., and Lam, K., “Investigations into water mitigation using a meshless particle method,” Shock waves 12(3), 2002, pp. 181-195.

42. Oregon State University. “O.H. Hinsdale Wave Research Laboratory,” http://wave.oregonstate.edu/facilities, last accessed 12/13/2018.

43. Linton, D., Gupta, R., Cox, D., van de Lindt, J., Oshnack, M.E., Clauson, M. “Evaluation of Tsunami loads on wood-frame walls at full scale.” In Journal of Structural Engineering ASCE, 2013;139:1318–25. http://dx.doi.org/10.1061/(ASCE)ST.1943-541X.0000644.